POLITECNICO DI TORINO

Master's Degree in Biomedical Engineering

Master's Degree Thesis

Optimization of machining process on electrospun nanofibers for integration in microfluidic devices

Supervisors

Prof.ssa Marzia Quaglio

Dr. Simone Marasso

Candidate

Licia Perri 254391

TORINO, July 2021

Table of Contents

Abstract

The main goal of this thesis is to fabricate a PDMS-based microfluidic Lab-On-a-Chip (LOC) with polyacrylonitrile (PAN) nanofibers inside the channels to facilitate micro-RNA (miRNA) capture. The designed and developed device is oriented, in a viral detection context, to the execution of tests with RNA immobilization and amplification with an isothermal amplification method.

The good properties of PDMS were exploited, namely the biocompatibility, the versatility and the stickiness it exhibits with a very wide range of materials, including polymer-type nanofibers. The main technological challenge was to integrate nanofibers inside the microfluidic channels, thus exploiting their intrinsic characteristics: high surface-to-volume ratio and high porosity per unit mass. These can substantially improve the performance of microfluidic devices addressed to virus detection, increasing their capture capability. A fabrication protocol was defined to allow LOC bonding in presence of the patterned nanofibers, which must be kept unaffected by the passage of test fluids and pass the leak tests. The reason why PAN was chosen for nanofibers deposition is related to the chemical nature of its surface, presenting amino groups which, activated by plasma treatments, facilitate the capture of miRNA. Another advantage is that PAN allows for the electrospinning of fibers in a controlled manner. As regards the layout, the LOC has a silicon base, on which nanofibers find place, and a PDMS top-cover which includes: a microfluidic channel concentration area (15.5 mm x 10.5 mm) with squared 500 µm x 500 µm channels; an inlet well for biological sample injection; an outlet for waste withdrawal. The layout of the device was designed using the software Rhinoceros® (Robert McNeel & Associates) by first making the 2D model CAD and then the 3D model. The master mold, subsequently used for the PDMS chip replication, was printed using a poly-jet 3D printer (OBJET 30 from Stratasys). Before depositing the PAN nanofibers, the silicon substrate was spin-coated with a layer of PDMS. Then, by laser ablation, the same geometry of the microfluidics was patterned on the deposited PAN nanofibers. The PDMS chip replica was bonded via interlayer bonding technique and leakage tests were carried out. Leak tests in ethanol (at 60 °C for 10 minutes) were conducted to verify that the bonding technique allowed for proper adhesion of the PDMS replica to the underlying substrate. At the end, interlayer bonding turned out to be the right assembly technique. Moreover, the overall process ensured a good alignment of the nanofibers as well as their stability, even after fluidic tests as demonstrated through microscopic characterizations.

This thesis work has been developed in the framework of a collaboration between the Politecnico di Torino-DISAT and Consiglio Nazionale delle Ricerche (Istituto dei Materiali per l'Elettronica ed il Magnetismo) and partially funded by the National grant VIRAD-C19 (Rilevazione VIrale RApiDa del COVID-19) FISR 2020 COVID (FISR2020IP_00044). The aim of this collaboration is to investigate a new rapid diagnostic tool for viral detection, specially addressed to robust detection of SARS COV-2.

1. Introduction

1.1 Structure and classification of the viruses

Viruses are small infectious agents (20 nm to hundreds of nm). They are not truly autonomous organisms as they can live and reproduce only within a host cell and do so by exploiting its functional mechanisms. The virus-infected cell can be of bacterial, plant or animal origin. Analyzing the structure of viruses it can be observed that it is very simple[1]: there is the capsid that represents the protein envelope, whose surface can be covered by the pericapsis which is a membrane that in turn is composed of a layer of glycoproteins and a phospholipid layer (Figure 1.1)[2]. Inside the capsid is enclosed the viral genome, which may consist of RNA or DNA, sometimes you can also find proteins that have the function to organize the genetic material and manage its replication within the host organism.

Viruses are classified according to:

- type of genome and its organization: there are DNA viruses, single-stranded or double-stranded RNA viruses, with circular, linear or fragmented genomes;
- structure and symmetry of the capsid (helical, spherical);
- presence of a pericapsid;
- size;
- site of replication within the host cell (cytoplasm, nucleus);
- infected cell type.

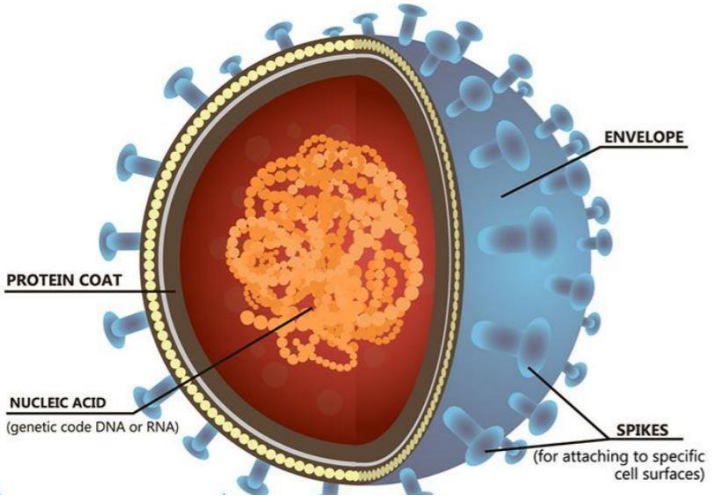

Figure 1.1- Structure of viruses[2]

As already specified the nature of the cells that are infected can be different, coronaviruses for example, single stranded RNA viruses can infect both animal and human cells. Their structure consists of a pericapside that has projections, which in turn have a glycoprotein, the so-called spike protein, which gives it a crown structure. The virus takes advantage of these projections to recognize specific receptors of the host cell, favoring their entry and therefore the development of the infection[3].

When viruses have not yet entered a cell they are known as virions, but because they are not autonomous organisms when in contact with the external environment they do not have the same ability to infect as when in the cell. In order to enter a cell, a virus uses its surface receptors, which bind to the cell membrane, and once inside the cell, it releases its genome and, using the host's replication system, multiplies very rapidly.

The replication process involves a series of steps[4] (Figure 1.2)[5]:

- adsorption-attachment of the virus to the cell membrane: in this step there is an interaction between the antireceptor of the virus and the receptor that is located on the surface of the host cell;
- penetration inside the cell: which can occur by fusion in the case in which the viruses of interest are equipped with pericapside that precisely merges with the membrane of the host cell, or by endocytosis that consists in the formation of vesicles that incorporate the virion;
- decomposition of the viral genome due to the degradation operated by lysosomal enzymes that degrade the envelope of the virus and then the viral genome is in direct contact with the cytoplasm of the cell that has been infected;
- replication of the viral genome and synthesis of viral proteins, but, in this phase a distinction must be made, because in the case of DNA viruses the replication of the genetic material takes place within the nucleus of the host cell, followed by the phase of transcription into RNA and then the synthesis of viral proteins. In the case of RNA viruses, however, the replication of the genetic material and the synthesis of viral proteins do not take place in the nucleus of the host cell but in its cytoplasm.

- Release, which can occur through mechanisms of exocytosis, or through cell lysis. Either way at this stage the now complete virions are released outside the cell.

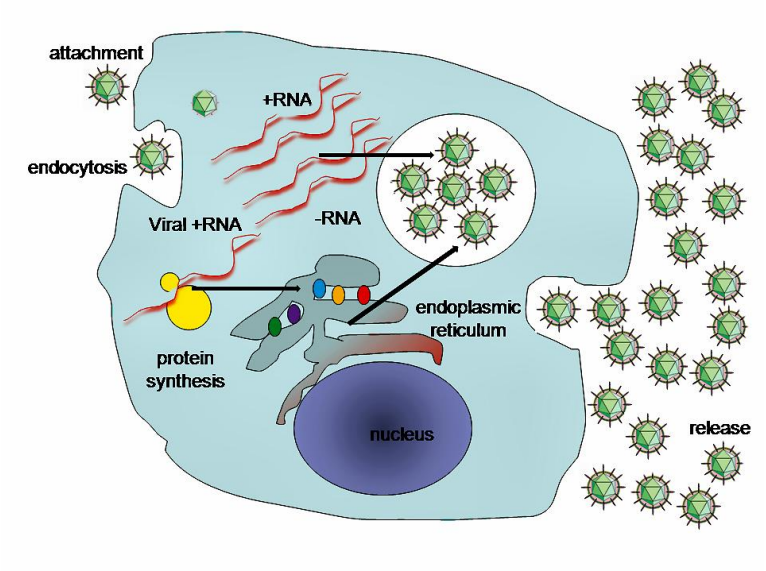

Figure 1.2 – Virion replication cycle[5]

- viral proteins and viral genome after the phases of synthesis and replication respectively are found in very high numbers, combine and give rise to a viral progeny that from the genetic point of view has the same characteristics of the starting virus. With processes of cell lysis, this progeny is released and spreads to other host cells in the body and at this point the cycle of infection and subsequent replication is repeated[6].

When the viral functions of a virus within the cell are not active, it means that the virus itself is in a latent state, so there is no formation of viral progeny and its spread within other host cells. However, as a result of external factors or cellular processes, viral functions can be reactivated resulting in the generation of infections.

Depending on the virus type, the infection can have different consequences for the host cell:

- it is destroyed and dies.
- it survives, but continuously produces small numbers of viruses and is chronically (persistently) infected.
- it survives and the viral genome remains in a latent state without producing infectious particles.

- it is immortalized, thus gaining the capability of unlimited cell division, a process that can be associated with malignant transformation into a tumour cell.

1.1.1 Replication mechanism of RNA viruses

Replication of viral genomes is accomplished by the RNA-dependent RNA polymerase (RdRp) that is specifically encoded by the virus[4]. Additional RNA strands are synthesized due to the viral RNA genome template. The replication process of RNA viruses results in the ability to synthesize three types of RNA: the genome, a copy of the genome, and mRNAs[4]. There are proteins that are critical for the production of the infectious genome, and the set of these proteins is known as the replicase complex, depending on the virus family of interest the number of these proteins will be different. In the context of synthesis, it is necessary to distinguish between mRNA synthesis and genome synthesis, in fact the proteins needed to synthesize mRNA are no longer proteins that are part of the replicase complex, but we talk about transcription complex[4].

RNA viruses can be divided into two groups, based on the viral genome: positive or plus (+)-strand RNA viruses and negative or minus (-)-strand RNA viruses[6], in particular, when we talk about RNA-positive viruses their genomes are functional mRNAs. After penetration into the host cell, assembly of ribosomes onto the genome for viral protein synthesis occurs. Synthesis of viral proteins requires penetration of the virus into the host cell and then ribosomes must assemble on the genome. Viral protein synthesis is important for the replication of RNA viruses because it allows mRNA and additional genomes to be synthesized[4].

When we talk about positive RNA viruses, during their replication they exploit cellular complexes with which they modify the cell membranes of host cells.

The transcription of negative RNA viruses occurs thanks to the action of viral proteins after the genome has penetrated the cell: they interact with the RNA proteins that are exposed by the capsid and bind to the genome[4]. Thanks to this interaction, it is possible to make the virus non-infectious by purifying the genomic RNA, if it is non-infectious the translation and consequently the transcription does not take place and

therefore it is degraded. The main steps for the genome to replicate are transcription and translation[4].

1.2 Conventional techniques for detection of viral diseases

Viral infections represent one of the global problems of our time, which is why detecting viral particles is of paramount importance. There are different approaches for the detection and identification of viruses, such as microbiological and biochemical tests, genetic engineering methods and immunological methods.

We can divide the methods for detection of viral particles into the following groups:

- detection of infected cell cultures[7];
- detection of viral antigens[7];
- detection of viral nucleic acids[7].

The practical use of these methods for the detection of viral particles is very significant, but at the same time they are expensive, complex and time-consuming. It is therefore important to develop new methods that are more effective and faster in solving the problems associated with the analysis of viral particles. Instrumental implementation of these methods should ensure high accuracy of measurements, and measurements should be carried automatically by mid-level personnel. An important criterion in the development of new methods for determining viruses is their versatility and the ability to use them for various purposes.

Detection on cell cultures is based on virus growth, isolation from cell lines, and identification of the virus itself based on the effects and changes it causes in host cells. Another method that also relies on cell culture is hemadsorption in which erythrocytes adsorb to the plasma membrane of infected cells. The cell culture technique, although a standard technique, is too time consuming, specifically about four weeks[7]. For this reason, an alternative method has been developed, i.e. rapid culture in clamshell vials: cells are grown on a slide, then the virus is deposited on this layer of cells, everything is then centrifuged at low speed and the virus is detected by immunofluorescence. While this is a rapid culture assay, it is not sufficiently sensitive. A very expensive and not very rapid method is electron microscopy (EM)[7]; It is a technique that allows an efficient identification of viral particles because it is based on their counting. The above-mentioned techniques were later replaced by more

sensitive and quantitative immunoassays that are able to detect virus antigen or antibodies in clinical samples. The high specificity and binding affinity between the antigen and the antibody have generated a number of immunoassays with different detection approaches. One of the most common methods is the enzyme-linked immunosorbent assay (ELISA), which, thanks to its double specificity, has become a gold standard for the detection of proteins[7]. Another rapid immunochemical technique for detecting the presence of a specific antigen is Later Flow, which operates on the same principles as enzyme-linked immunosorbent assays (ELISA).

The problem with immunoassays is the possibility of giving false negative results due to the window period between viral infection and subsequent antibody production. This time window varies between viruses, but the increased sensitivity of NA-based methods has revolutionized virus diagnostics by shortening the window period and thus decreasing the likelihood of false negative results[7]. There are several techniques that can directly detect viral-specific DNA or RNA by in situ hybridization, dot blot or Southern blotting, but the limitation of these techniques is their insufficient sensitivity[7]. In this regard, there are techniques with higher sensitivity that rely on NA amplification and detection. In addition to standard PCR, there are variants such as quantitative PCR (qPCR) for DNA and RT-PCR for RNA, and both are becoming important for assessing viral load[7]. However, there are some significant drawbacks to implementing these molecular techniques in the field: DNA extraction requires elaborate protocols to allow nucleic acid purification; equipment was too expensive. Instead, it is important that methods for viral diagnosis in the field be sufficiently sensitive and specific, simple and rapid, with results that are easy to interpret, and should require as little equipment as possible[8].

In recent years, to solve the problems of diagnosis in the field, research has focused on the isothermal amplification technique, which refers to all methods in which the DNA amplification reaction takes place at a constant temperature. This offers advantages in terms of simplicity over classical PCR, as the reaction does not need to undergo several temperature cycles. In addition, isothermal reactions use enzymes that can efficiently replicate large amounts of DNA.

1.2.1 PCR (Polymerase Chain Reaction) and some of its variations

The polymerase chain reaction (PCR) has been developed since the 1980s and has revolutionized the diagnosis of genetic and infectious diseases. The technique allows to obtain a very large number of molecules identical to the stretch of DNA that has been chosen to be amplified, whose initial and final nucleotide sequences are known, even from extremely small amounts of starting nucleic acid[9].

A variety of techniques have been developed that build on the original PCR method: real-time PCR, also known as quantitative PCR (qPCR), combines PCR amplification and detection in a single step; RT-PCR known as reverse transcription polymerase chain reaction, which starts with RNA as a template for nucleic acid. It starts with a mixture that contains the DNA template that has the sequence of interest, primers, nucleotides, and DNA polymerase and PCR subjects this mixture to cycles of heating and cooling[10]. The primers, after cooling, bind to the target DNA by exploiting the complementary bases that allow pairing. Through the primers the DNA polymerase creates the new complementary strand.

The phases of which a PCR cycle is composed are as follows[10] (Figure 1.3):

I. denaturation of the double helix of the template DNA into two single helices at a temperature of about 95°C to break the hydrogen bonds;
II. annealing of primers to complementary single-stranded DNA sequences located at the end of the target fragment, at temperatures between 50°C and 70°C. They must be complementary to the 3’ ends of the anti-parallel strand of the template DNA;
III. extension of the primers in the 5'-3' direction by the addition of nucleotides by DNA polymerase, finally leading to the synthesis of a new helix equal to the starting DNA template, at temperatures between 68 and 72°C.

After the extension step, the reaction returns to the denaturation step and PCR continues. With each cycle the amount of DNA is doubled, in particular there is an exponential increase as each new DNA strand serves as a template for replication in the following cycle[10].

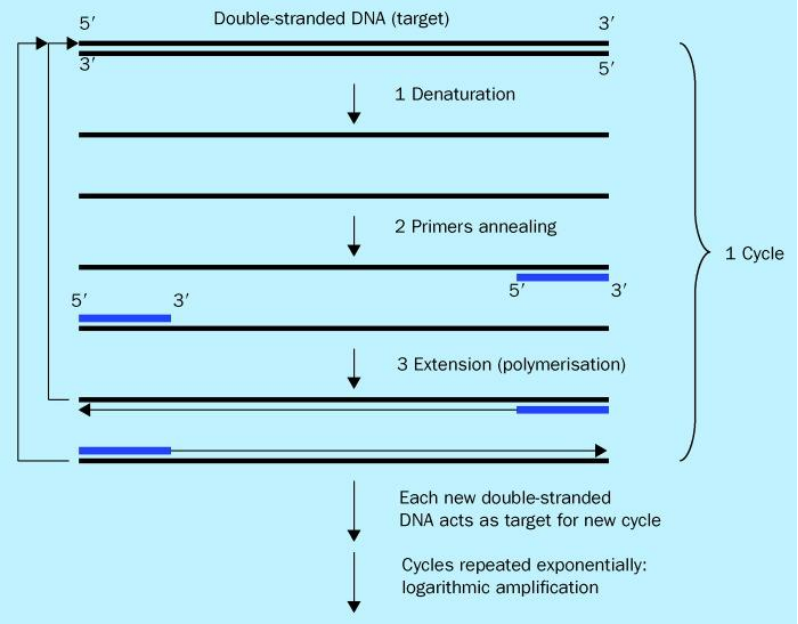

Figure 1.3- Schematic of PCR reaction[10]

Among the variants of PCR mentioned above, those that are widely used in molecular pathology applications are RT-PCR and real-time PCR.

What is ultimately obtained is complementary DNA (cDNA), which is more stable than RNA because it is not degraded by RNase. In RT-PCR, upon degradation of the starting RNA, double-stranded DNA (dsDNA) is produced and then PCR amplification continues in the traditional manner. RT-PCR is widely used to diagnose and quantify RNA viral infections and in the analysis of mRNA transcripts such as those occurring in non-Hodgkin's lymphomas, leukemias and sarcomas[11].

A significant advance in PCR technology is quantitative real-time PCR, which combines amplification and detection, facilitating real-time amplicon detection. For this purpose, a fluorescent signal, generated during amplification, is incorporated into the amplicon and detected with a specialized thermal cycler. Fluorescent signals are generated during amplification[12].

Real-time PCR and conventional PCR differ for the following reasons:

- Real-time PCR does not require post-amplification treatments, this reduces the risk of amplicon contamination;
- the results of real-time PCR are more reproducible;
- Real-time PCR systems are able to perform melting curve analysis, which provides greater specificity for detecting unknown sequence variants[12].

The practical advantages of real-time PCR over conventional PCR mainly include speed, simplicity, reproducibility, and quantitative capability[13].

1.2.2 LAMP (Loop-mediated isothermal amplification)

In vitro amplification of nucleic acids is a central technique in biotechnology and molecular biology and is currently one of the most widely used methods in clinical diagnostics. In this regard, PCR was the first technique of nucleic amplification to be developed and it is still the most widely used in diagnostics.

However, PCR has several limitations[14]:

- cost, because it requires advanced and expensive equipment.
- there is a risk of contamination.
- is sensitive to inhibitors and contaminants.
- it requires specialized personnel to both perform the technique and interpret the results.

The limitations described above have led to the development of alternative methods, particularly isothermal amplification techniques, i.e., reactions that take place at a constant temperature. One of the techniques that has achieved great popularity is loop-mediated isothermal amplification (LAMP).

LAMP has the following advantages:

- it uses simple and inexpensive instruments.
- it allows to amplify and visualize the product within the same tube.
- amplification takes a short time because no initial DNA denaturation is required.
- it is characterized by high sensitivity[15]
- combined with reverse transcription it is able to detect the presence of a target RNA[16].

This method is based on the synthesis of DNA through strand detachments and cyclic amplifications that take place at constant temperature, by means of a highly efficient DNA polymerase and a set of two internal and two external primers. The inner primers are called Forward inner primer (FIP) and Backward inner primer (BIP) respectively and each contains two sequences corresponding to the two directions of the target DNA (3'-5',5'-3')[17], one to trigger the reaction in the first step and one in

the second (Figure 1.4). The target sequences of these two primers are named as follows: the parts at the outer ends are F2c and B2 and the inner ends F1c and B1 respectively. At the outer end of the target sequences for FIP and BIP are two other regions, the binding sites for the other two primers F3 and B3[18]. The reaction, which is carried out in 30 minutes at a constant temperature of 65°C, begins when part of the FIP primer attaches itself to the F2c target sequence and starts to replicate[19]. At the same time, the external F3 primer, which is shorter than FIP and present in a lower concentration, attaches to the F3c site and begins to detach the replicate strand from the FIP primer. Part of the BIP is then attached to the target sequence (B2c) of this replication and replication begins[18]. In the meantime, the outer B3c sequence is attached to the outer B3 primer, which detaches the replicated strand. This first part of the reaction leads to a ring shape of the replicated DNA[19]. This, with the attachment of the FIP and BIP primers to the sides, is immediately converted into a shape similar to half of the first and from here the second stage of the reaction begins, leading to exponential amplification of the DNA obtained[19]. The final products of the amplification reaction are a mixture of DNA with forms with single loops and arms of different lengths and forms with multiple loops resulting from annealing of inverted repeats of the target sequences that were in the same strand[17].

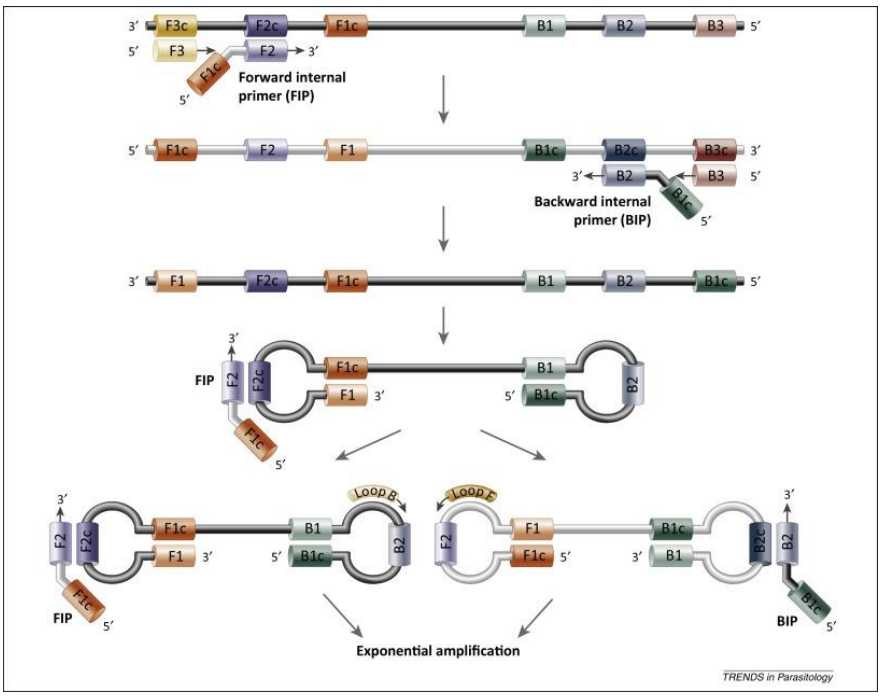

Figure 1.4 - How the LAMP reaction work[18].

Due to its advantages, LAMP represents one of the most valid methods for the rapid diagnosis of infectious diseases. It is a simple technique that is used in clinical laboratories in developing countries because it requires little elaborate and therefore inexpensive laboratory equipment. It is currently used in applications such as detection of pathogenic bacteria, detection of metastatic cancer cells20 and pathogenic viruses. The LAMP technique is widely used for the detection of DNA viruses but especially RNA viruses[20], [21], in some cases it manages to be more sensitive than PCR. A very recent use is that of RT-LAMP in the detection of SARS-CoV-2 and it has been demonstrated that it is able to provide results as sensitive, specific and especially cheaper than those provided by PCR which is considered the "gold standard".

1.2.3 LFA (Lateral Flow Assay)

Lateral flow tests (LFAs) are low-cost, simple, rapid, and portable detection devices. This type of test has attracted considerable interest because it can offer patients with an immediate diagnosis[22].

The lateral flow assay (LFA) is a paper-based platform for the detection and quantification of analytes in complex mixtures, where the sample is placed on a test device and results are displayed within 5-30 minutes. LFA-based assays are widely used in hospitals, medical offices, and clinical laboratories for the qualitative and quantitative detection of specific antigens[23] and antibodies and also gene amplification products. Samples that are used in this technique are blood that is drawn from the fingertips, saliva, urine, and fluids taken via nasal swab. The principle of operation is as follows: a liquid sample containing the analyte of interest moves through various areas to which molecules are attached that interact with the analyte. On the other hand, from the point of view of components, a lateral flow test strip (Figure 1.5) is characterized by overlapping membranes mounted on a support in order to provide better stability and handling.

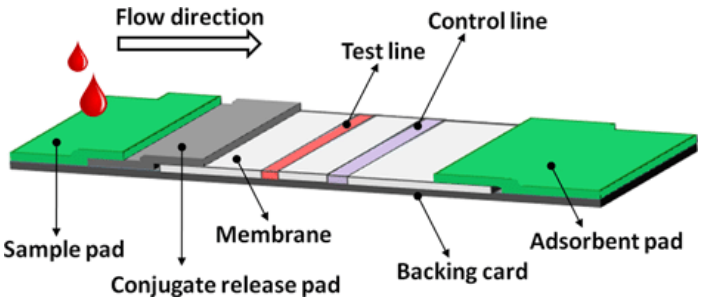

Figure 1.5 – Typical components of LFA test strip[25]

Typically, the LFA consists of the following elements[22]: sample pad, conjugate release pad, membrane with immobilised antibodies and adsorbent pad. The mechanism of LFA is explained below: the sample is applied to the adsorbent pad which in turn contains surfactants and buffer salts that allow the analyte to bind to the membrane. Next, the sample migrates through the conjugate release pad, which contains antibodies specific to the target analyte. The analyte binds to the conjugate antibody and the sample continues to travel to the detection zone, which is a porous membrane consisting of specific biological components, typically antibodies or antigens, that are immobilized in lines that react with the analyte, which is in turn bound to the conjugate antibody[24]. When the sample analyte is recognized there is a response on the test line and one on the control line indicating that the flow is correct along the strip[24]. This test is based on the capture of conjugate-antigen colour complexes by the antibody, which is immobilised on each line. The number of lines present on the strip increases as the concentration of the analyte increases[24,25]. Liquid is able to flow through the dispositive by capillary force and reflux of the liquid is prevented by the presence of the absorbent buffer, whose task is to absorb excess reagents.

1.2.4 ELISA (enzyme-linked immunosorbent assay)

ELISA is an acronym derived from enzyme-linked immunosorbent assay. It is a versatile immunological assay method used in biochemistry to detect the presence of a substance (antigen) using one or more antibodies to which an enzyme is bound: the enzyme is bound to the antibody in such a way that neither the catalytic properties of the enzyme nor the antibody specificity are altered[26]. This method of

investigation falls into the category of enzyme immunoassays. ELISA applications can be used to diagnose a number of viruses including Zika virus and Syphilis[27].

The enzymes used catalyse reactions whose products are coloured and can therefore be detected even in very low quantities by colorimetric reading on a spectrophotometer. There are different variants of the ELISA test, which differ according to the component that is to be detected. In the direct test, the presence of the direct or sandwich ELISA antigen is determined, in the indirect test, the presence of specific antibodies against the antigen[28].

In the direct assay process, the antigen is trapped between two layers of antibodies and, for this reason, this method is also known as sandwich ELISA (*Figure 1.6*). The sample is added to the wells of a polystyrene microtitre plate, which has previously been coated with antibodies specific for the antigen being sought. If the antigen, which may be a virus, bacterium or protein, is present in the sample, it will be captured by the binding site exposed by the antibodies immobilized in the plate. After removing the unbound material by a series of washes, a second enzyme-conjugated antibody is added. The second antibody recognizes a different antigenic determinant on the same antigen. Following further washing, the amount of antigen originally sequestered in the reaction is determined by adding the enzyme substrate[29]. The amount of enzyme product, made evident by the production of a colour, is proportional to the amount of antigen captured.

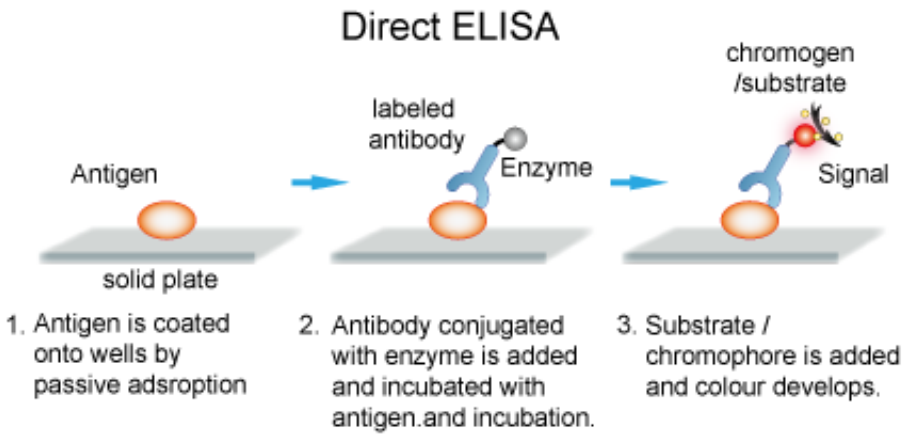

Figure 1.6 – Direct ELISA flowchart[30]

In contrast, the indirect ELISA test is used to detect antibodies in human serum (*Figure 1.7*). To perform an indirect ELISA, microtitre plates are coated with an antigen preparation. The dilutions of the patient's serum are added gradually, the mixture is then incubated to allow for the binding of antigens to specific antibodies. A specific antibody is added to detect antigen-antibody complexes. The antibody that is added later is the combination of human Igg and an enzyme. After that, the intensity of color detected allows to detect the enzymatic activity following the addition of the substrate31. The colour obtained is proportional to the number of antibodies present in the serum that have recognised plate-bound antigens. So when you create this kind of bond between antigen and antibody, it means that the patient has come into contact with the virus. This type of test corresponds to an indirect ELISA test, which is currently the test that is used for HIV detection in seropositive people.

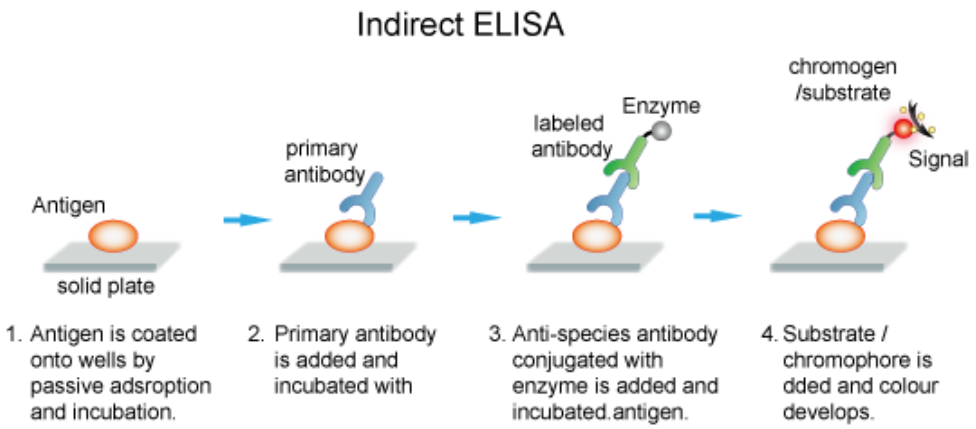

Figure 1.7 – Indirect ELISA flowchart[30]

1.3 Lab on chip to detect viruses and some clinical application

Conventional methods, as described in the previous paragraph, used for the diagnosis of viral diseases involve cell cultures that are infected by the virus, or are based on the detection of viral antigens, antibodies and nucleic acids, all of which necessitate high kit costs, a lot of work by well-trained operators and, above all, are not able to provide timely results[7].

The technological innovation was made possible by so-called Lab-on-a-Chip devices (LOC). A LOC is a device of just a few square centimeters that can perform all the functions of a true human-scale scientific laboratory, such as transferring samples,

taking a precise volume of reagent or mixing two reagents, and many more[32]. Conventional laboratory processes often require large volumes of reagents to perform an analysis, and if the test sample is too small there is a risk that it will be diluted so much that it will cancel out any associated signal, making it impossible to detect. On the other hand, the small size of a LOC allows small quantities of reagents to be used when performing trials, so a small sample size will still result in a high concentration and therefore a good signal.

Basically, the main advantages associated with a microfluidic system are as follows[33]:

- Very low capacities of samples and reagents
- Cost-effective
- Can perform multiple reactions simultaneously
- Shorter analysis times and faster results
- High resolution and sensitivity in the detection and separation

Each integrated microfluidic device features a set of microfluidic elements, each of which is associated with specific functions such as reagent storage, fluid transport and mixing, product detection, and ultimately collection.

Recently, lab-on-a-chip (LOC) technologies are highly exploited in the field of virus detection, making it possible to detect viruses competently[34]. However, after detecting a specific virus, it is necessary to understand all its features, including its subtypes and genotypes in order to proceed with the most appropriate treatment.

The following will review some viruses of interest in recent years and discuss the application and performance of microfluidics employed for their detection.

1.3.1 Influenza virus

Influenza is an acute infectious respiratory disease caused by the influenza virus, an RNA virus of the Orthomyxoviridae family. Studies carried out by the World Health Organizatione show that about 5-15% of the population is infected by influenza viruses and that the number of deaths is between 25.000-500.000 each year[35]. Flu symptoms can range from mild to severe, the most common being fever, sore throat, muscle and joint pain, headache and general malaise. In severe cases of influenza, viral pneumonia, secondary bacterial pneumonia and worsening of pre-existing

health problems can also be observed. Symptoms usually appear two days after exposure to the virus and last less than a week. There are three genera of influenza viruses: Influenzavirus A, Influenzavirus B, Influenzavirus C. Each genus includes only one species: Influenzavirus A, Influenzavirus B and Influenzavirus C. Viruses A and C infect several species, while virus B infects almost exclusively humans[36]. A and B viruses have 2 glycoproteins on their surface: haemagglutinin (labelled H) neuraminidase (labelled N). Inside the envelope are segmented single strand RNA and nucleoprotein (NP). Depending on the surface glycoproteins, virus A is subdivided into subtypes. Specifically, it can be presented in 144 different subtypes based on combinations of 18 haemagglutinins (H1 to H18) and neuraminidases (N1 to N11)[37]. There are several conventional methods for diagnosing the influenza virus. These include viral culture and subsequent immunocytological analysis of the viral antigen. After 2-10 days of viral culture, clinical laboratories use rapid immunological tests for virus detection, such as the direct immunofluorescent test or the membrane enzyme-linked immunosorbent test[38], possibly followed by characterization by serological or molecular biological methods. It is a very versatile technique, which can identify various respiratory viruses, but has a major limitation in terms of the time needed to obtain results (4-10 days). In addition to viral culture, the use of complement fixation (CF), haemagglutinin inhibition (HI) and PCR is common[39]. CF is based on the property of complement to react in the presence of antigen-antibody complexes, 'fixing' it and not making it available for other reactions. The test consists of adding to the test serum, which is the serum of the patient in contact with a specific antigen, a 'detector' serum consisting of red blood cells sensitized with antibodies, which cause hemolysis of the red blood cells in the presence of the available complement. If hemolysis does not occur, the complement has already been fixed by the antigen-antibody complex in the test serum, so in this case the reaction is positive, which means that the specific antibodies to the antigen used in the test were present in that serum[40]. The haemagglutination inhibition test is a serological test used to identify certain viruses that can cause blood agglutination. These viruses have receptors on their surface, the hemagglutinins, which in turn bind to the surface of red blood cells, and the test is based on the use of antibodies that bind to the hemagglutinins of the virus and prevent it from binding to red blood cells. The hemagglutination test

requires the use of: serum containing antibodies that can react specifically with the hemagglutinins of a particular virus, the virus to be identified, and red blood cells with receptors for the virus. If the virus binds to the specific antibodies, it will not be able to bind to the red blood cells and there will be no hemagglutination, but if the virus and antibody do not bind, there will be hemagglutination and thus red blood cell sedimentation.

Both of these methods are sensitive and reliable, but require experienced personnel and laboratory time. RT-PCR is the most commonly used diagnostic test as a tool to identify influenza virus infections, but mainly for virus detection, typing, and subtyping[41]. The technique consists of extraction of viral nucleic acids from clinical samples, cDNA synthesis by in vitro reverse transcription of viral RNA triggered by specific synthetic oligonucleotides corresponding to known nucleotide sequences on viral genes and subsequent amplification of cDNA with specific primers and DNA polymerase. Methods used to detect the amplified product may include fluorescence and luminescence measurements. RT-PCR is a faster, more sensitive and specific test than the methods described above, but disadvantages include cost, a high false-positive rate and a complicated procedure[42].

Recently, microfluidics represents a promising technology for the detection of influenza virus in order to have faster and more accurate methods of diagnosis. Over the years, various microfluidic devices have been proposed by different research groups for influenza virus diagnosis. In 2016, an integrated microfluidic method based on the sandwich aptamer was developed by Lee's group that could detect H1N1 within 30 minutes[43]. In 2019, Ma et al. created a very simple microfluidic device that integrates nucleic acid extraction and RT-LAMP providing colorimetric detection of results within 40 minutes[27],[44]. More recently, Shen et al. more recently made a microfluidic chip that takes advantage of a glycan coating on magnetic beads to capture the virus by exploiting the RT-PCR method. The microfluidic device just mentioned is examined in more detail below.

In this work, an integrated microfluidic system was developed that combined the advantages of microfluidics and RT-PCR to automatically perform the entire process of influenza virus detection and subtyping[45]. Based on the high specificity between influenza viruses and glycans, glycan-coated magnetic beads were used as probes to

first capture all influenza viruses in a sample. Viral typing (InfA and InfB) and HA × NA array subtyping with one-step RT-PCR using different combinations of universal virus primers and HA- and NA-specific primers in the array reaction chambers of the microfluidic chip[45]. With this approach, up to 12 InfA subtypes could be simultaneously detected in an automated manner in less than 100 min on this microfluidic platform[44]. The dimensions of the microfluidic device are 84 mm (length) × 59 mm (width) × 10 mm (depth) and consisted of a thick film polydimethylsiloxane air control layer, a thin film PDMS liquid channel layer, and a glass substrate to seal the microfluidic chip[45]. Briefly, these PDMS layers were fabricated by a standard soft lithography process, and the PDMS layers and glass substrate were bonded together by oxygen plasma treatment[45]. Several microfluidic devices were integrated into the microfluidic chip, including consecutive, pneumatically driven micropumps for liquid transport, a pneumatically-driven, open-type micromixer for sample and bead incubation, pneumatically-driven and normally closed microvalves for liquid control, air inlets, a waste outlet, air microchannels, liquid microchannels, loading chambers for liquid storage, overflow chambers for excess liquid storage, and RT-PCR chambers[45] (Figure 1.8)

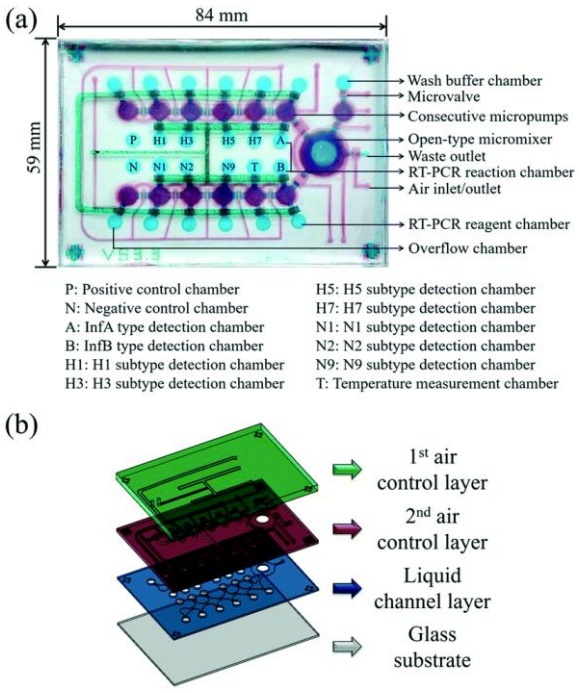

Figure 1.8 – microfluidic device for 12 influenza subtypes detection[45]

The loading chambers comprised one wash buffer loading chamber and 12 RT-PCR reagent loading chambers45. The latter 12 involved chambers for positive controls, negative controls (deionized distilled water), the temperature measurement, InfA typing, InfB typing, HA subtyping (H1, H3, H5, and H7), and NA subtyping (N1, N2, and N9)45. With these chambers, it was possible to identify up to 12 subtypes of InfA virus on the chip, moreover since the device incorporates a measurement and optical detection system it is possible to perform virus detection and subtyping and detect the respective signals. The schematic of the entire virus detection and subtyping process is shown in *Figure 1.9*. Figure 1.9a shows the loading step of the glycan-coated beads, virus sample, RT-PCR reagents and wash buffer. Figure 1.9b shows virus isolation using the glycan coated beads during mixing in the micromixer. Next, wash buffer is added to remove waste while a magnet is used to collect the complexes that have formed between the virus and the microparticles (Figure 1.9c). Figure 1.9d shows the resuspension in the wash buffer of the captured viral complexes, and then the release of viral RNA following thermolysis, lasting 5 min, achieved by the presence of a thermoelectric cooler that was placed at the bottom of the chip (Figure 1.9e). Subsequently, the liquid phase in which the viral RNA is present is transported to the RT-PCR reaction chamber (Figure 1.9f). The next figure shows the amplification of HA- and NA-specific genes by RT-PCR and finally the detection of fluorescent signals45 (Figures 1.9g and 1.9h).

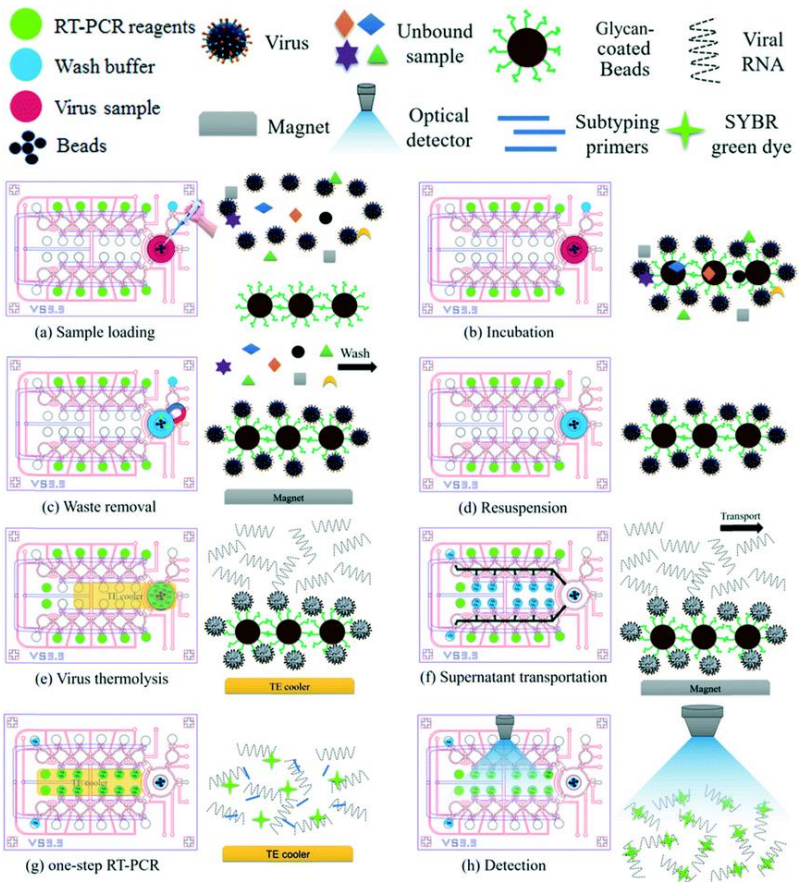

Figure 1.9 - Schematic diagram of the internal process of influenza virus detection[40]

It was possible to automate the virus subtyping process to also the detection process through the integration of a custom control system, this allowed for a reduction in the detection limitations (LOD) of the device compared to those of technologies already in the field[45]. From the results it was possible to observe that the device realized allows to perform tests in a fast and sensitive way, and could be suitable for point-of-care diagnosis[45].

1.3.2 ZIKA virus

The Zika virus (ZIKV) is a single-stranded RNA virus of the Flaviviridae family, first isolated in 1947 in Uganda. In humans it causes a disease known as Zika fever, which is structurally similar to the viruses that cause dengue, yellow fever and West Nile fever. Zika virus infection is usually asymptomatic, but can cause fever, rashes, joint pain, or conjunctivitis; during pregnancy it can cause microcephaly which is a severe birth defect, eye abnormalities, and a number of developmental disorders called

congenital Zika syndrome[46]. The vector is mosquitoes of the genus Aedes, and transmission of the Zika virus to humans generally occurs through the bite of the vector mosquito. Inter-human contagion is possible and known routes of transmission are saliva, urine, semen, breast milk and sexual transmission[47]. Globally, more than 2 million humans have contracted the Zika virus because of its high contagiousness, and it has recently been discovered that it can cause Guillain-Barre syndrome[48]. These data have highlighted the need for early diagnosis of the Zika virus. Reverse transcriptase quantitative polymerase chain reaction (RT-qPCR) is a gold standard method for viral RNA detection, but there remain limitations, such as the requirement for sample purification, expensive equipment, and well-trained personal, as well as the slow processing of results[49]. It is in recent years that microfluidics has been considered the appropriate and effective tool for rapid diagnosis, and it is in this context that microfluidic devices based on nucleic acid detection are to be found, and there are several applications among them.

Ganguli et al, (2017) produced a microfluidic chip that is based on the combination of RT-LAMP and smartphone. This chip has the ability to detect in multiplex ZIKV and other viruses offering accurate results[27]. The LOD of this system is $1.56e^5$ PFU/mL in blood under 35 min[50],[27]. Kaarj et al, (2018) made a paper microfluidic device combined with a smartphone to detect ZIKV RNA with RT-LAMP that is sensitive and highly specific. The limitation of these devices is that they require several purification steps. Yang et al, (2019) developed a microfluidic device capable of detecting the virus using the RPA (recombinase polymerase amplification) method for rapid and visual detection of nucleic acids. This system features a sensor, similar to a wearable bandage, which is activated by human epidermal heat (30°C-37°C)[51] precisely because RPA can react at room temperature[27]. It is an inexpensive, convenient and easy-to-implement method that can detect 10 copies/µL within 10 minutes[27].

In this study, flexible materials that have a low Young's modulus have been exploited and are specifically used to make wearable sensors that offer good skin contact. This technology was combined with the isothermal nucleic acid amplification method to create the wearable microfluidic sensor based on Ecoflex, which is a flexible material and, as mentioned earlier, is activated by human body heat and allows for rapid, visual and portable nucleic acid detection. The Ecoflex sensor was fabricated by soft

lithography exploiting a silicon master made by mechanical microfabrication. It consists of input and output structures (Figure 1.10 A) and a collection reservoir that allows instant readout. More in detail, it consists of a bilayer stack of two flexible and biocompatible low modulus silicone elastomers, in particular it is possible to recognize: a softer and adhesive layer based on Ecoflex in contact with the skin and another substrate of Ecoflex sealed by PDMS which is another silicone elastomer. By subjecting the flexible sensor to torsion, flexion and elongation tests, its flexibility was demonstrated (Figure 1.10 B). These characterizations were performed through mock element analysis (FEA)[51] and demonstrated that these sensors can be placed directly on the skin ensuring perfect contact.

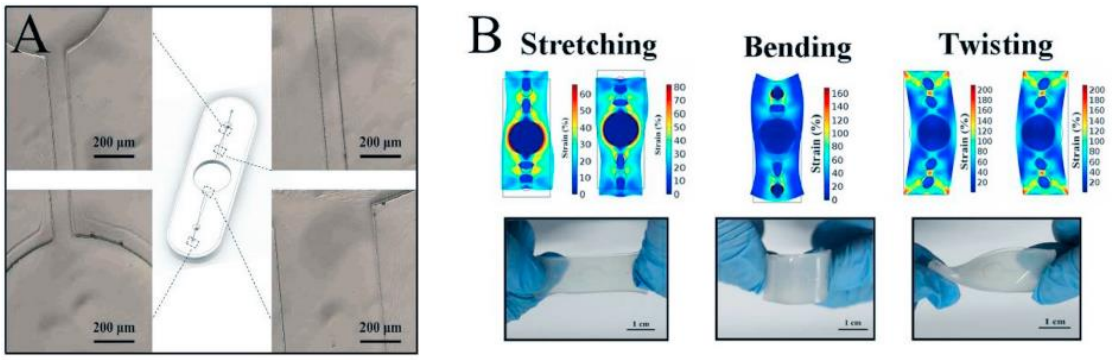

Figure 1.10 - Stress distributions on the device under stretching, bending, and twisting stresses[51]

The sensor under analysis consists of inputs, outputs, and a reservoir that allows instant display of the result. The fluid is controlled by a microsyringe and when it is put into operation, the inlets and outlets are sealed with a tape to prevent the fluid from escaping. RNA extraction from human serum is done using a commercial kit and once extracted, cDNA transcription is performed[51].

Before inserting the samples inside the sensor, they were processed and then added inside the reservoir. Next, the flexible microfluidic was sealed with a PDMS replica by plasma treatment. During the visual analysis process, RPA premixed reaction solution was placed inside the tank with a syringe and the inlets and outlets were sealed with tapes[51]. The sensor was placed on the human wrist via an adhesive layer for 10 min. Through a mini UV-vis flashlight, the fluorescent results could be viewed and using a smart phone as a detector, photographs were recorded[51].

The difference with PCR is that RPA does not require the denaturation process to achieve nucleic acid amplification.

From the results that have been obtained, it has been found that this wearable sensor allows for results within 10 minutes by taking advantage of a mini UV flashlight, can be exploited for the detection of pathogens once placed in situ, such as in the presence of wounds, and also for the diagnosis of cancer biomarkers in vivo[51].

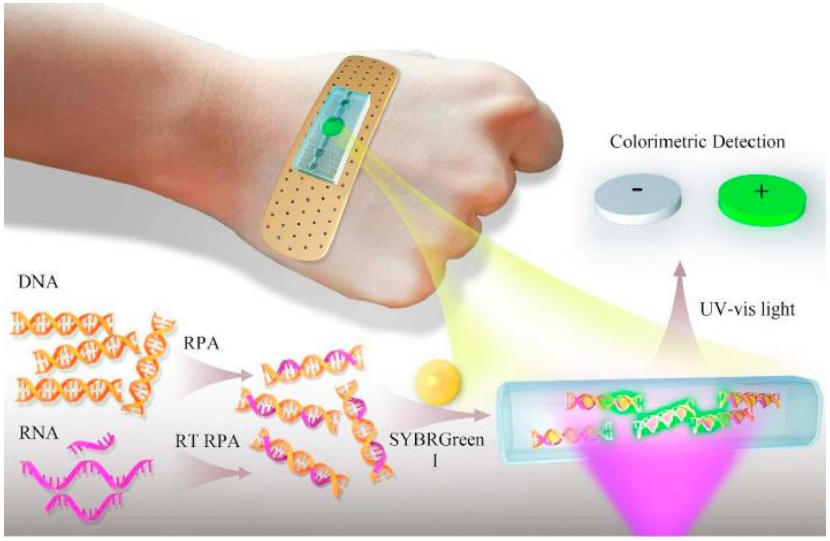

Figure 1.11 - Representation of the wearable microfluidic system[51]

2. Aim of the study

In the present work, a microfluidic Lab-on-a-Chip with integrated nanofibers, based on polyacrylonitrile (PAN), has been realized. In particular, the technological challenge was to integrate the nanofibers directly into the microfluidic channels of the device, optimizing a procedure for bonding the chip with the patterned nanofibers that would ensure a good resistance of the nanofibers themselves to the passage of fluids at different speeds. In order to realize this innovative system, the polymer selected to obtain the nanofiber layer was PAN, whose surface chemistry, characterized by amino groups that can be activated after plasma treatment, facilitates the capture of miRNA. Another advantage of this polymer is that it guarantees the formation of controlled nanofibers.

3. LOC fabrication technologies and nanomaterials integration for improved microfluidic diagnostics

3.1 Lab on a chip manufacturing methods and materials

In the introduction, it was explained that LOCs can carry out a number of analyses in the biomedical field and beyond. Each of these devices must be made from a material that meets specific requirements. for example, the properties of transparency to light of a certain wavelength, stiffness to avoid deformation of the can be required, such as transparency to a given wavelength of light, rigidity to avoid deformation of the channels under the effect of a liquid injected at high pressure, resistance to a certain solvent. The material from which a LOC is made partly determines the manufacturing technique, cost factors and the need to ensure particular characteristics in the device structure.

In this thesis work, the fully exploited material for the realization of the microfluidic device is polydimethylsiloxane (PDMS). PDMS is one of the elastomers that is most

widely used in the fabrication of microfluidic chips, due to its properties of elasticity, biocompatibility, permeability and especially for its surface chemistry that makes it highly hydrophilic[52]. It is precisely for these properties that it is exploited for the realization of microfluidic devices designed for applications in the biomedical sector. In this regard, the research group with which the device that is the subject of this thesis was created, Marasso et al., has already developed a PDMS microdevice for the purification and analysis of miRNAs and it has also been successfully tested[53].

The device is composed of a drop-shaped PDMS chamber (made using the mold casting technique) that once cured is assembled on a silicon support previously coated with PDMS through a spincoater. The assembly is done through a plasma oxygen treatment. For the capture of miRNAs the surface of these PDMS devices has been subjected to silanization, thanks to the chemistry of PDMS that makes it suitable for surface functionalization.

From the clinical point of view, it has been shown that some miRNAs are directly involved in the development of certain diseases and are therefore used as biomarkers. In this study, a fluorescently labeled miR-21 was exploited, it was placed in contact with the surface of the PDMS device in order to evaluate the adsorption and elution on both functionalized and non-functionalized surfaces. It was found that the functionalized surfaces showed a greater tendency for adsorption and elution, in contrast to the non-functionalized surfaces where they were much less pronounced. Furthermore, these abilities were tested over time, and it was seen that the functionalized devices maintained their adsorption performance more or less unchanged for three months, confirming their stability[53].

Next, the possibility of performing both purification and miRNA analysis on the chip was evaluated. In this regard, validation was performed on plasma, sera and solid tissues. Although different chemistries were used for reverse transcription and amplification, miRNAs were successfully purified and analyzed, showing better results in the presence of functionalized surfaces.

The results showed that PDMS microfluidic devices could be introduced in clinical applications, ensuring the possibility of easy, fast, compact and above all low-cost assays.

In this context, a way to further improve the functioning of the system was considered with regard to miRNA capture, in particular by increasing the surface area. To achieve this goal, it was considered to integrate nanofibers and as explained in Chapter 2, the technological challenge was just to integrate them inside the microfluidic channels of the designed PDMS device.

3.2 Integration of nanofibers in microfluidic systems

Currently, the gold standard for the detection of protein biomarkers within biological samples or viruses and bacteria is the ELISA assay, along with a number of conventional methods that have been described previously. Among the disadvantages of these techniques are: low sensitivity, high costs, long analysis time and large amount of sample required, do not allow a rapid and sensitive diagnosis of diseases[54]. Taking advantage of the progress made in recent years in the field of nanotechnology and microfluidic technology, it has been possible to develop diagnostic methods that overcome the limitations of conventional methods: they allow a faster analysis at lower costs, an early diagnosis and are characterized by greater sensitivity[55]. On the one hand, microfluidic devices allow for the precise control and manipulation of small amounts of fluid moving through the action of capillary forces[56], require low volumes of samples to be analyzed, have a high portability and the time required for processing is reduced. Thus, compared to conventional devices they allow rapid diagnosis at low cost. On the other hand, there are nanomaterials, with sizes between 1 and 100 nm, which due to their unique characteristics such as high surface-to-volume ratio, their tendency to be easily chemically modified, show superior detection sensitivity[57]. By combining these two technologies, with their associated advantages, significant developments in disease diagnosis and medical therapy can be achieved, enabling the creation of systems suitable for future clinical applications. In this regard, for the realization of these highly sensitive biosensors, several nanomaterials have been used, among them nanoparticles, nanotubes and nanofibers[54]. In general, the requirements that must be met by a biosensor are different: first of all they must be non-toxic, they must provide an accurate response, they must be highly specific, they must be effective

and at the same time inexpensive. Biosensors differ from each other on the basis of a number of parameters: the technique used to manufacture them, the type of receptor[58] that they use in the detection phase and on which the level of selectivity depends, the type of transducer that translates the biorecognition phenomenon into a measurable effect. Recent developments in nanotechnology have made it possible to improve biosensors from a sensing perspective[59]. This has been made possible by introducing nanomaterials into these systems, because a nanoscale geometry of the adopted materials has been shown to positively influence sensing activity. Recently, among all the possible nanostructures to be used in biomedical diagnostic systems, nanofibers have gained great importance. Thanks to their intrinsic properties such as high specific surface area and large pore volume per unit mass, they have allowed to manufacture and market biosensors with high sensitivity and selectivity.

Another advantage of integrating nanofibers with microfiber devices is that it allows to overcome some limitations of nanofibers including the low mechanical strength that prevents their use in other applications. The main function of electrospinned fibers, integrated into a microfluidic device, is to act as a substrate to increase the surface area available for specific immobilization of analytes or as a selective filtering media, all while increasing sensitivity. In addition to improving the sensitivity and detection activity of biosensors, nanofibers also influence other aspects, such as capture, culture[60] and release of specific cells and analyte concentration.

In the present thesis work, as explained above, a microfluidic Lab-on-a-Chip with integrated nanofibers, based on polyacrylonitrile (PAN), was constructed to facilitate the capture of miRNAs.

3.2.1 Materials

Historically, the first material used for the manufacture of Lab-on-a-chip was silicon, due to its high surface stability and thermal conductivity and good resistance to organic solvents[61]. The chemistry of its surface, based on the silane -Si-OH group, is well developed and therefore modifications can be made to reduce non-specific absorption or improve the conditions for cell cultures. Today, silicon is little used due to the high cost of the manufacturing process (photolithography) and its opacity to visible light, which prevents its use in applications requiring the detection of

fluorescence light emitted by the sample[62]. Another material used for the manufacture of LOCs is glass, which has good surface stability and thermal conductivity, is biocompatible and chemically inert, and has a modulus of elasticity in the range of 50-90 GPa, which limits its use in some applications. Glass is transparent to visible light. The main problem, in common with silicon, is the cost of processing by photolithography. The need to overcome the limitations of these two materials has paved the way for the use of polymers, because they make it possible to set up microfluidic systems quickly, economically and by reducing the risk of contamination of samples[63]. One of the great advantages of polymeric materials is the fact that there are so many of them, with different mechanical, chemical, physical, optical and electrical properties. This, combined with the existence of numerous microfabrication methods, makes it possible to select the optimum material for a given application.

The subdivision of polymers into thermoplastic, thermosetting and elastomeric materials[64] depends on their physical properties and also on the manufacturing technique that is adapted to work them. This subdivision is made on the basis of certain parameters, among which are the glass transition temperature (T_g) which is the temperature below which a polymer is brittle while above it becomes plastic again; the thermal distortion temperature (HDT) which is the temperature at which it is possible to stress a polymer for a short period and provides useful information on its thermal properties, beyond this temperature the polymer cannot be subjected to any mechanical stress otherwise it would yield; the decomposition temperature (TD) which is the temperature at which the decomposition of the polymer takes place. Thermosetting polymer materials consist of cross-linked polymer chains. When the polymer undergoes heat treatments or is exposed to radiation it cross-links, once the polymer is cross-linked it can no longer be processed because it takes on a hard three-dimensional structure. This is the reason why if you go to subject this inflexible and cross-linked structure, which is nothing more than a thermosetting polymer, it will undergo decomposition but we will not obtain a melt[65]. There are several thermosetting materials that are used for the realization of microfluidic devices, among them the photoresist SU-8[65], that is very thermally stable, resists many solvents and is transparent to visible light. The cross-linking of this material occurs

after exposure to UV light, the cross-linking causes the chains to bind together with very strong bonds so the material becomes very fragile[65].

Thermoplastic polymers are formed by non crosslinked and weakly bonded chains when their glass transition temperature is exceeded they become soft and easy to work materials. However, following numerous heating and remodeling processes, the polymer degrades from a thermal point of view and therefore has a consequent reduction in its starting qualities[66].Each time the material is heated, and the reshaping operation is repeated, there is a certain degree of thermal degradation and therefore it loses some of the quality characteristics it had originally. The most commonly used thermoplastics materials for the production of microfluidic device are polymethylmetaacrylate (PMMA), polycarbonate (PC), polystyrene (PS), polyvinylchloride (PVC), polyimide (PI) and cyclic olefin polymers (COC and COP)[67]; Table 3.1 shows their relative Tg. Thermoplastic polymers have proven to be suitable for the mass production of LOCs due to some important properties: they have a modulus of elasticity in the order of GPa, have a higher resistance to solvents, absorb little water, are transparent in the visible light and have a low autofluorescence.

	PMMA	PC	PVC	PI	COP	COC
$T_g(°C)$	110	148	100	90	138	78

Table 3.1: Tg of some thermoplastic polymers taken from[67].

Elastomers are materials endowed with a high elasticity, this means that during the application of a stress, for example a traction stress, they change a lot their dimensions and then once removed the stress they recover the deformation going back to their original dimensions. One material that is widely used in microfluidics is poly(dimethylsiloxane), also known as PDMS[67], it is a very cheap material, easy to work with machines that are not sophisticated, it is a biocompatible material and transparent to the visible light. The properties of this material will be discussed in more detail.

3.2.1.1 Poliydimethylsiloxane (PDMS)

Polydimethylsiloxane, called PDMS, is the most widely used elastomer for the fabrication of microfluidic devices. It is a mineral-organic polymer with a structure that contains carbon and silicon, belonging to the siloxane family. The empirical formula of PDMS is $(C_2H_6OSi)_n$ and its fragmented formula is $CH_3[Si(CH_3)_2O]_nSi(CH_3)_3$, n being the number of monomers repetitions[68].

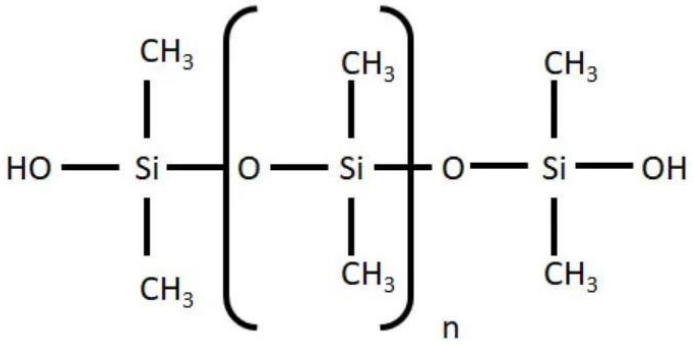

Figure 3.1 – Molecular structure of PDMS[68]

Depending on the value of n, we can distinguish a nearly liquid PDMS if n is low, or a semi-solid PDMS if n is high. This distinction can be made when the PDMS is in a non-crosslinked form. Due to the presence of siloxane bonds, the chain is extremely flexible and has viscoelastic characteristics. In the cross-linked form, on the other hand, PDMS presents itself as an elastomer with hydrophobic characteristics. The cross-linking can take place at high temperatures, hundreds of degrees, in a shorter time, but it can also take place at room temperature and last longer. PDMS is characterized by a glass transition temperature of -125°C.

For the fabrication of microfluidic devices, PDMS (liquid) mixed with a cross-linking agent is poure into micristructured mold and heated to obtain a elastomeric replica of the mold.

PDMS is characterized by a number of properties that make it a very attractive polymer from a biomedical perspective: it is biocompatible, has good thermal stability, is transparent, has low surface tension, is very stable, is an inert material, has a low elastic modulus, and is inexpensive[69]. In order to make microfluidic devices it is mixed with a cross-linking agent and since it remains liquid for many hours at room temperature it can be easy to process. it is characterized by good optical

properties for both light transmission and fluorescence microscopy and has elastic behavior[69].

For applications in microfluidics, PDMS is characterized by its gas permeability, elastic behaviour and surface properties.

Permeability: PDMS has a much higher permeability than other elastomeric materials, but in the context of cell cultures this could cause pH changes due to carbon dioxide diffusion and could also lead to evaporation. One way to reduce the permeability of this polymer is to increase the concentration of crosslinker with which it is mixed.

Elasticity: the good elasticity of PDMS is associated with the sliding of the adjacent chains, in fact in normal conditions, the chains assume a wrapped conformation, when the material is subjected to a load they stretch and once the load is released they return to wrap. Obviously, the more the PDMS is cross-linked the less elastic it will be.

Surface properties: PDMS as a result of its surface chemistry, which has methyl groups, is a highly hydrophobic polymer so it has poor wettability in the presence of water and this promotes non-specific adsorption of proteins.

Also due to its surface chemistry, PDMS is able to bond well to glass substrates or other PDMS layers simply by performing plasma treatment. This is an extremely advantageous property in the context of microfluidic systems because it allows for very stable assemblies.

However, using PDMS has some limitations that have not yet been resolved:

- specific adsorption problems;
- possible swelling in the presence of apolar solvents;
- permeability to small hydrophobic molecules;
- problems during assembly due to slow thermal hardening;
- 1% reduction in cross-linking;

3.2.1.2 Polyacrylonitrile (PAN)

Polyacrylonitrile (PAN), is a vinyl polymer characterized by a number of important properties such as solvent resistance, abrasion resistance, is a polymer that has high thermal and mechanical stability and high tensile strength. PAN can be used in

numerous application areas such as composite materials, nanosensors, biochemical purification, and biomedical application[70]. Most acrylonitrile polymers are obtained by continuous processes in aqueous suspension or in solution. In suspension polymerization, the monomers are dispersed by agitation in an aqueous solution of the catalyst. The suspension containing the monomer and catalyst is maintained at the polymerization temperature (700°C) to form the polymer, which is insoluble in the aqueous medium in which the reaction takes place[71]. The polymer is separated by filtration and washed to remove impurities.

More specifically, polyacrylonitrile is obtained from acrylonitrile, which is the starting monomer, having formula C_3H_3N consisting of a vinyl group bonded to a nitrile - C≡N. The polymer is obtained by radical polymerization using as initiator a peroxide or a mixture of potassium peroxydisulfate $K_2S_2O_8$ and a reducing agent such as potassium hydrogen sulfite KHSO_3.

The scheme of the reaction is represented in Figure 3.2[72].

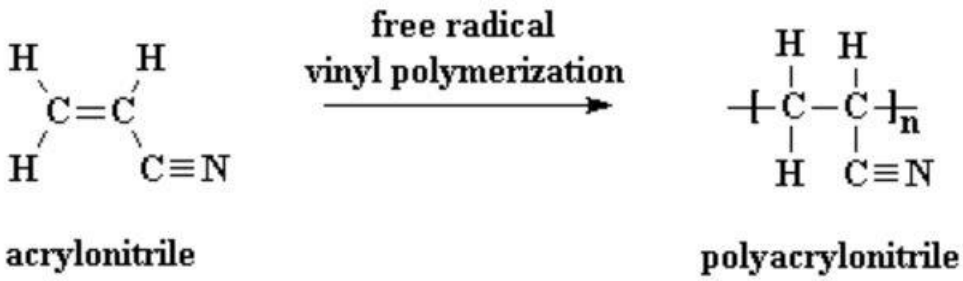

Figure 3.2 - Radical polymerization reaction to obtain polyacrylonitrile[72]

Polyacrylonitrile fibers are characterized by a density of 1.17 g/cm^3 have an insulating power, present an elongation at break of 15%, are characterized by good thermal stability and resist well to dilute alkaline solutions[72].

3.3 Fabrication of Lab-on-a-chip

There are several techniques that are used to fabricate Lab-on-a-chip and they can be classified into: direct fabrication techniques if the technique allows you to directly produce the device and then there are replication fabrication techniques that allow you to produce a negative copy of the device you want to fabricate. Examples of

direct manufacturing techniques include micro-milling[73], 3D printing[74], and clean room machining[75]. With all of these techniques, at the end of the process you get the final device made of exactly the same material that was used from the beginning. Direct fabrication techniques are very fast, in the sense that they allow us to observe immediately what is the result of the replica, as soon as it is produced, and if changes in the structure are needed they are done in a short time. The limitation of these techniques is that when faced with the production of a large number of devices, weeks may be necessary. In this case, it is preferable to use the replication manufacturing techniques that are based on the realization of a master which is used to obtain the replicas and it is not necessary to go to each production process to reproduce the entire structure. In some cases, techniques belonging to the class of direct fabrication, such as micro-milling, are exploited to make the master of the device of interest. Then once the desired structure is obtained, which is nothing more than the "negative" of the device one can exploit the PDMS elastomer that is poured inside the mold, it is left to cross-link and once ready it is detached and one can proceed with the realization of another replica. A widely used technique to fabricate polymer-based microfluidic devices is hot-grooving: the polymer is melted above your glass transition temperature (Tg), poured into the mold, and pressure on the order of MPa is applied under vacuum conditions for a short time on the order of a few minutes. At the end of the process, you cool the system and peel off the replica. Another widely used technique when polymeric LOCs are to be made is injection molding[66]: the polymer of interest in the form of dried powders is melted at a temperature above its Tg, the melt is injected into a closed mold and pushed through a high-pressure screw into the cavity of the master. Once the polymer is solidified it is detached from the master and the replica is obtained.

3.3.1 Soft lithography

Soft lithography is a family of techniques that use an elastomeric mold, among these techniques the one we will focus on and usemeo for the fabrication of the device that is the subject of this thesis is replica molding. Conventional lithography and soft lithography are based on the same principles, but the latter is able to overcome

limitations. The process on which soft lithography is based consists of a series of steps[76] *(*Figure 3.3)[77]:

- deposition of a uniform layer of a light-sensitive organic polymer, commonly called photoresist, on the semiconductor substrate by spin coating;
- overlay of a photolithographic mask having the desired pattern;
- exposure of certain parts of the photoresist to ultraviolet (UV) light or electron beams according to the pattern of the mask protecting certain areas;
- removal of the photoresist from the regions exposed (in the case of positive photoresist) or unexposed (in the case of negative photoresist) to the beam of photons or electrons, by immersion in a special development solution, leaving the mask pattern etched in the photoresist.

Mainly this technique is used to obtain replicas of PDMS[78], so since it is a very elastic material with a low stiffness, during the extraction phase of the replica the mold is not subject to mechanical or thermal stress that can ruin it, reason why it is possible to use the same mold to make a few hundred replicas.

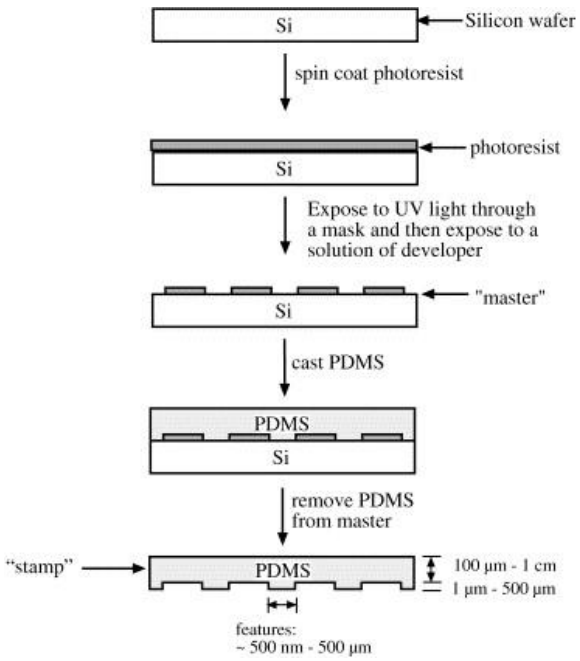

Figure 3.3 – Soft lithography[78]

As explained, the process of replica molding allows to duplicate what is the structure of the mold in negative obtained by lithography. Typically an elastomer is used, which is mixed with a crosslinking agent, the mixture is poured into the mold and then

allowed to cure either at room temperature or through heat treatment. A parameter that influences the resolution of this process is the structure and geometry that characterize the master.

In many cases, to obtain microfluidic systems, after obtaining the replica this is bonded on substrates, which can be for example glass, so as to create channels through which to pass test fluids or biological samples and then make the subsequent measurements and experiments. In order to obtain a tight seal and improve the adhesion between the device and its substrate, surface treatments are performed[79] (Figure 3.4).

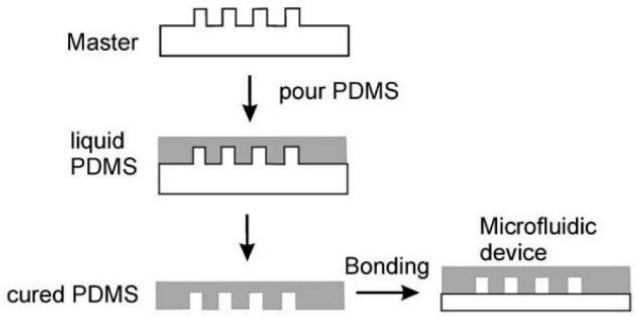

Figure 3.4 – Replica molding[80]

3.3.2 3D printing

3D printing is a technique defined as "additive", because it allows to obtain an object by depositing the material of interest layer by layer until the complete realization of the structure. There are several additive techniques, among these two widely known are the fused deposition modeling and stereolithography, and all in order to realize the final object start from a CAD model that is made before the manufacturing process, this CAD model is given dough to the machine that goes to convert the file in an STL extension and then allows to realize the print by depositing layers successively one on the other.

3.4 Description of electrospinning process

The electrospinning technique allows nanofibers to be extruded through the needle of a syringe, which is loaded with the polymer solution of interest, thanks to the application of an electric field. Thanks to the application of this electric field the

molecules acquire a certain charge that allows them to overcome the surface tension of the solution and at a certain point they come out of the needle, a jet of solution is formed which is deposited on a collector and this is guaranteed by the fact that during the spinning process the evaporation of the solvent takes place. The components required for electrospinning are as follows (*Figure 3.5*)[80]: a syringe that contains the polymer solution, a pump that controls the flow of the solution exiting the syringe, a voltage generator that is in turn connected to the syringe needle via an electrode and finally there is a metal collector on which the fibers are deposited.

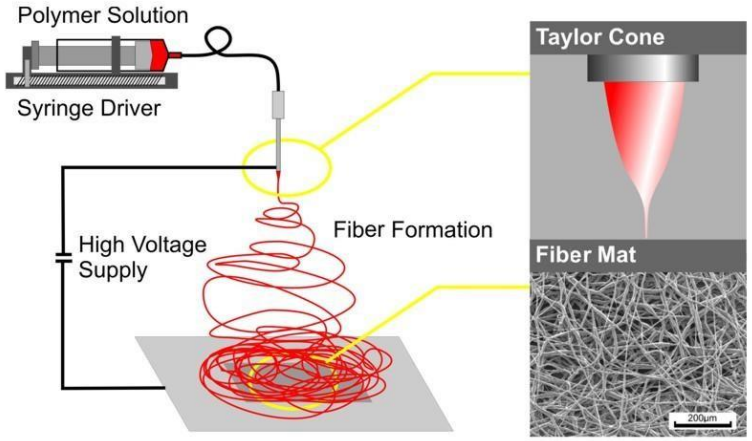

Figure 3.5 - Electrospinning scheme[80]

Let's see the process in detail: in order for the polymer solution to flow out of the syringe needle, the electrical potential must exceed the characteristic value of the solution itself and at that point the solution flows out and a cone[81] is formed, known as Taylor cone. This cone is formed because of the accumulation of electric charges that repel each other and this causes at a certain point to exceed the surface tension and viscosity of the solution itself[82]. Downstream of the cone a linear jet is formed which subsequently undergoes instability phenomena leading to its progressive thinning, generating filaments with a section that can be between one micrometer and one nanometer. During the journey of the jet occurs the evaporation of the solvent, to arrive at the end to impact and deposit on the collector connected to the ground and completing the electrical circuit. Because of the chaotic motion to which the jet is subjected, the fibers are deposited in a random manner, generating a disorderly interweaving of fibers in which porosity is present

3.4.1 Effects of various parameters on electrospinning

There are many parameters that influence the electrospinning process and the morphology of the fibers, which can be droplet, pore or smooth (*Table 3.2*). These can be classified into two categories:

Solution parameters	Environmental parameters	Processing parameters
Concentration	Temperature	Fluid flow rate
Polymer molecular weight	Humidity	Voltage bias
Viscosity		Needle diameter
Solution conductivity		Needle-to-collector distance
Surface tension		

Table 3.2 – Parameters that influence electrospinning process

3.4.1.1 Solution parameters

The solution parameters mainly influence the morphology of the obtained fibers. The parameters shown in (Table 3.2) are analyzed below.

- Concentration: this is a parameter that greatly influences the morphology of the fibers, in particular the presence of defects, to obtain fibers that are free of defects the concentration must assume useful values. A solution with low concentration will be characterized by a discontinuous saying, in particular drops will be formed and then collected on a metal collector[83]. On the contrary, a solution with a higher concentration will be characterized by the presence of defects, which have the shape of pearls[84]. As the concentration varies, the morphology of the defect also varies, in particular the higher the concentration the more the defects become thinner[84].
- Polymer molecular weight: this parameter influences the viscosity of the polymer, the higher the molecular weight the higher its viscosity. It has also

been observed that as the molecular weight increases, the diameter of the fibers that are electrospun and deposited on the collector also increases.

- Viscosity: influences the ease of production of the fibers, because with a high viscosity there is a risk of blocking the syringe nozzle[85] because the solution flows with great difficulty, but at the same time a too low viscosity affects the morphology of the fibers which risk not being able to maintain the shape once deposited and to collapse on themselves
- Solution conductivity: Increasing the conductivity of the solution means increasing its charge, consequently the charges within the jet repel causing the fibers to elongate and thus decrease in diameter[85]. If instead the conductivity is low the Taylor cone is not formed[84], therefore there will be defects that will have the shape of pearls. The use of salts [86] or solvents[87] more conductive allows to increase conductivity.
- Surface tension: once the electrical charge exceeds the surface tension of the polymer solution, the jet is generated which allows the fibers to be produced. In order to avoid that during the process, drops are formed as a result of the opposition of the surface tension, it can be considered to use a solution that is characterized by a high viscosity in order to overcome the surface tension[88].

3.4.1.2 Processing parameters

In order to obtain defect-free fibers, care must be taken to select the right process parameters as well as the materials to prepare the solution to be spun. The parameters shown in Table 3.3 are analyzed below:

- Fluid flow rate: this parameter influences the speed at which the jet is ejected from the nozzle and consequently the speed of the jet during the travel before settlling on the collector[89]. A low flow rate facilitates complete evaporation of the solvent[90] A greater flow rate affects the diameter of the fibers, favoring an increase and also an increase in porosity, but this could favor the formation of defects that have the shape of beads[91].
- Voltage bias: the applied potential influences the formation of the Taylor cone and therefore the subsequent expulsion of the jet from the nozzle of the syringe, to make this happen its intensity must exceed a certain threshold the generation of the fibers.

The threshold value depends on the polymer you are using[84]. Studies have found that increasing the electric field increases the likelihood of beads formation[85], and reduction in fiber diameter, because the forces of repulsion between the charges inside the solution increase[85],[84].

- Needle diameter: this parameter strongly affects the diameter of the fibers and consequently their size. In fact, the smaller the internal diameter of the spinneret, the smaller the diameter of the fibers. There is a lower limit below which the solution just cannot flow through the nozzle and this occurs mainly in the case where you want to electrophile solutions that have a high concentration and therefore a high viscosity.
- Needle-to-collector distance: this parameter influences both the morphology of the fibers and their diameter, because the speed with which the evaporation of the solvent depends on it. The greater the distance between the needle and the collector, the smaller the diameter of the fibers, but if we approach them beyond a certain limit, defects are produced and the size of the fibers increases.

3.4.1.3 Environmental parameters

Another class of parameters that influences electrospinning is that of environmental parameters, specifically the temperature and humidity present in the environment in which the process is being carried out. These two parameters are closely connected to each other, because a high temperature reduces humidity, and low humidity causes the solvent to evaporate faster[90].

- Temperature: indirectly affects the diameter of the fibers, because it affects the rate of evaporation of the solvent and the viscosity of the solution which, as mentioned above, greatly influence the size of the fibers. The temperature value is closely related to the polymer you choose, so in order to keep a certain solution liquid the values to set will be different.
- Humidity: relative humidity influences not only mechanical properties that are related to stiffness, and thus fiber diameter[92], but also solvent evaporation and the possible presence of pores[83]. In general, an increase in this parameter leads to the formation of thick[90] superficially porous fibers[85], which can evolve into heterogeneous fibers affected by beads, if it increases

too much[92]. On the other hand, low humidity speeds up solvent evaporation[85] and gives the fibers a smooth and homogeneous surface[92].

4. Materials and methods

This chapter reports the techniques and materials used to fabricate the microfluidic device and the subsequent characterizations performed for experimental validation.

4.1 Device design

The chip layout was designed using a 2D model by Rhinoceros® software (Robert McNeel & Associates), followed by a 3D STL model prepared with the same CAD. This modeling software is based on a NURBS mathematical model that allows 2D and 3D geometries to be represented precisely through a user-friendly interface. The microfluidic device made in this thesis project exhibits a morphology that we see in Figure 4.1.

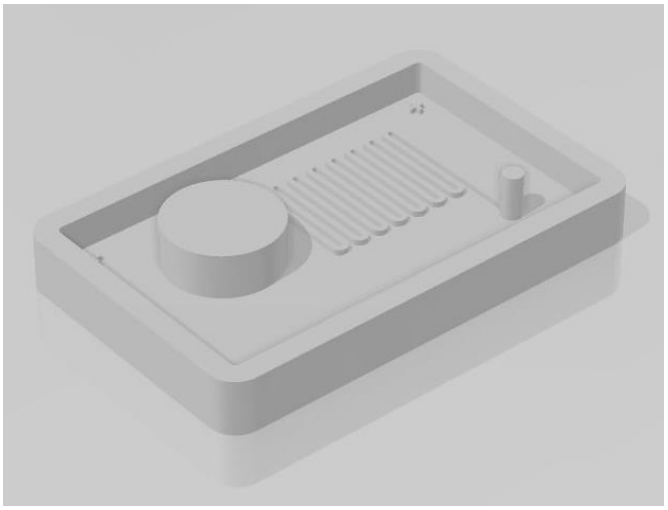

Figure 4.1 - The morphology of LOC device

The layout of the device includes a microfluidic channel concentration area that has a size of 15.50 mm x 10.50 mm, where the nanofibers were subsequently deposited, a well that represents the inlet for the insertion of the biological sample, and an outlet where the sample is aspirated (Figure 4.2). The diameters of inlet and outlet are 10.00 mm and 1.80 mm, respectively. The microfluidic channels have a 500 µm x 500 µm square cross section with a 500 µm gap separating them from each other. Aligners represented by 4 crosses placed at the corners of the device have been realized in order to facilitate the alignment for the next bonding step. Everything was enclosed within a frame of size 37 mm x 22 mm, which subsequently allowed us to make the mold to obtain the replicas.

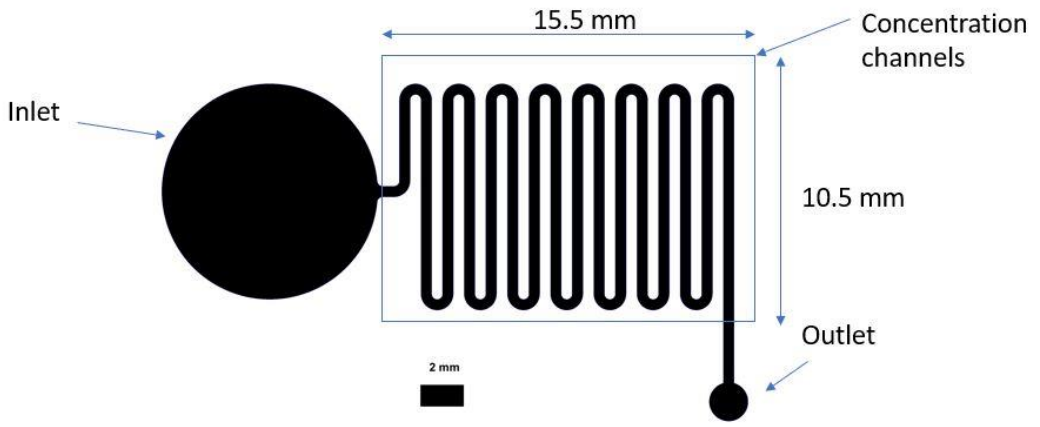

Figure 4.2 - Device layout that is composed by: concentration channels, inlet and outlet.

The realization of this layout started with the realization of the 2D model (Figure *4.3*), using the software mentioned above, which shows us the measures and dimensions described.

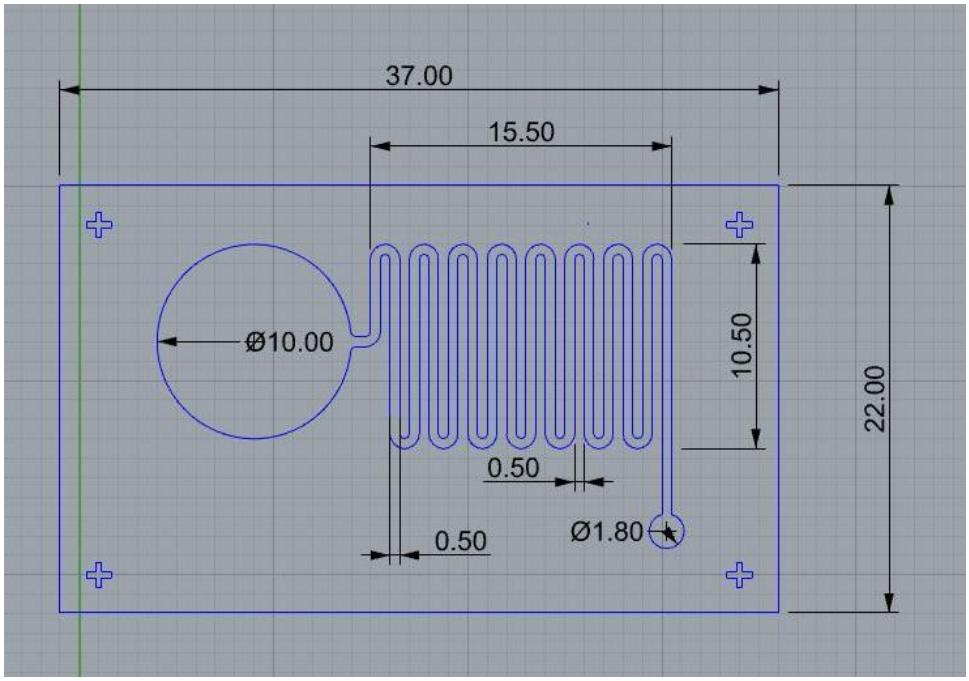

Figure 4.3 – Top view of the 2D model in which the geometric measurements are reported in millimeter scale

The 3D layer of the LOC device was constructed from the 2D layer. To make the design, the individual parts were extruded individually as closed surfaces. Then, the individual features were merged to obtain the whole chip (Figure 4.4).

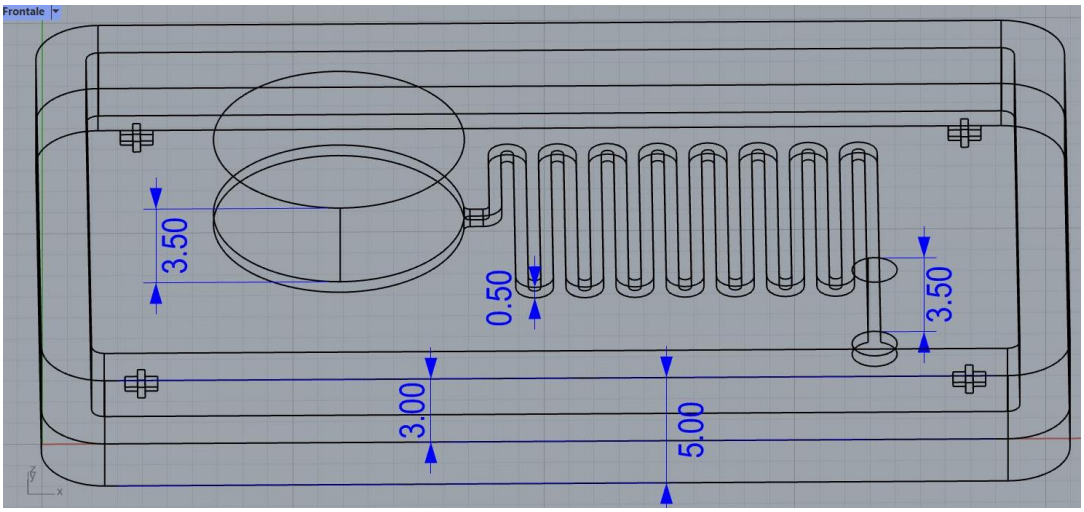

Figure 4.4 - Front view of the 3D drawing with dimensions of the extrusions in millimeter scale

With respect to the base plane, the extrusion measurements for the various components are as follows: 0.5 mm for the microfluidic channel concentration area, 3.5 mm for inlet and outlet, 3 mm for the frame. The reason why the extrusion of inlet and outlet is higher than that of the frame is related to the fact that in correspondence of these we wanted to obtain holes in the replication phase, to allow the insertion and aspiration of the various test fluids. Within the microfluidic channels, excluding inlets and otulets, the total volume of test fluids that can be contained is 41µl.

4.2 Device fabrication

The manufacturing process of the entire device can be summarized in five steps: 3D printing of the master, manufacturing of the device by replica molding technique, functionalization of the silicon substrate, patterning of the nanofibers, and sealing of the device by special bonding technique. A fabrication that can be considered easier and faster than conventional micromachining techniques.

4.2.1 3D printing of the master

The master of the microfluidic device was fabricated with the 3D printing technique, specifically using a poly-jet 3D printer (OBJET30 Stratasys) (Figure 4.5)[93] characterized by an excellent printing resolution and that also allows, the use of many materials[94]. The printer software is able to convert the STL format file of the final CAD. The drawing is converted to a low-level language that can be interpreted by the machine. In particular, by means of optimized slicing algorithms, it is possible to split the imported 3D geometry into two-

dimensional slices, so that the final part is constructed layer by layer, combining inkjet technology with the photopolymerization process.

Figure 4.5- Chilab 3D printer

There is a pre-processing phase, in which, thanks to the Objet Studio software the part is oriented on the construction tray of the printer. This is followed by an elaboration phase in which drops of liquid photopolymer VeroWhite™ (from Stratasys) are deposited on the tray by means of an inkjet head, along the XY plane, and each layer solidifies thanks to the presence of a UV lamp that promotes polymerization. At the end of each layer, the tray lowers along the Z axis and continues with the deposition of subsequent layers until the part is complete. As mentioned earlier, the printer allows you to use a wide variety of materials, each with different properties. The mold was fabricated using two polymers: a structural resin provided by Stratasys (the mentioned VeroWhite™) and the second polymer was used as a sacrificial material (SUP705) to support the structure during device fabrication (Figure 4.6).

Figure 4.6 - 3D printed mold

The duration of the printing was about an hour, at the end of which the piece obtained was removed from the tray, with the help of a spatula and a jet of water was used to remove the support material and was left in the oven at a temperature of 95 ° C for 24 hours that the material to promote the curing of the resin. In order to obtain a perfectly clean surface that would guarantee an excellent performance of the molding process, the master was subjected to heat treatment in the ultrasonic bath; in particular, it was closed in a container containing acetone, placed in the bath for 5 minutes by selecting the appropriate parameters: frequency equal to 65KHz, temperature equal to 20°C and a power of 100%.

4.2.2 Microfluidic devices production

The material to produce the microfluidic devices was PDMS, obtained from SYLGARD®184 that is a silicone-based elastomeric kit that is a two-component system with a polymer base and a curing agent that cross-bonds with the polymer matrix.

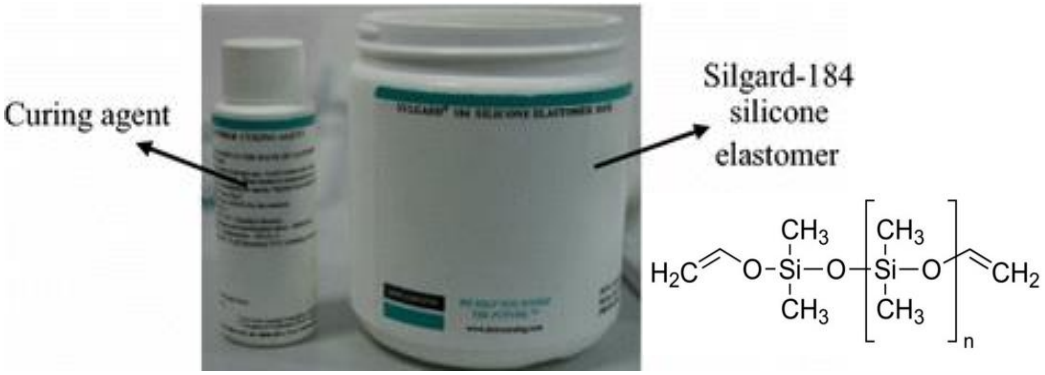

Figure 4.7- PDMS SYLGARD 184 and *its* chemical structure[52]

Sylgard 184 silicone elastomer is especially useful for applications where clarity is desirable. The PDMS solution was prepared by mixing the polymer base and curing agent in the ratio of 10:1 volume/volume (v/v), respectively. The two different substances were mixed under hood, inside a container, for a few minutes to form a homogeneous mixture. The air incorporated during mixing was removed by placing the still uncrosslinked PDMS inside a vacuum pump until the bubbles completely disappeared. After degassing the solution, a thin layer of silicone mixture was poured inside the rigid master and the degassing operation was repeated. After degassing the solution, a thin layer of silicone mixture was poured inside the rigid master and the degassing operation was repeated, because after several tests it was observed that especially in correspondence of the loops of the microfluidic numerous air bubbles were formed, which once the entire mold was filled, could not be eliminated. After filling the mold with the silicone mixture, it was placed in an oven at a temperature of 95°C for one hour to allow cross-linking to occur. After cross-linking, the replicas were removed

from the mold with the help of a small spatula by inserting ethanol between the replicas and the molds to facilitate detachment.

4.3 Physical characterization of the microfluidic device

After fabrication, characterizations of both the chip and the supporting substrate were performed by exploiting digital microscopy and field emission scanning electron microscope (FESEM) to investigate physical characteristics such as dimensions and surfaces.

4.3.1 Digital microscope characterization of the device

With the aim of analyzing the geometry of the channels on the PDMS replica, measuring the distance between them, evaluating their heights and investigating their dimensions, the digital microscope Leica81 was used, using the dedicated software LAS VA.1 (Figure 4.8).
In this regard, a horizontal cut was made in the replicas to measure the heights, so that the section could be evaluated. What we wanted to investigate, in particular, was the distribution of the heights of the channels: being the replica molding performed on a levelled plane what we wanted to achieve was a distribution as homogeneous as possible of the heights, in order to promote optimal bonding with the substrate support and in order to precisely align the channels with the pattern made on the nanofibers.

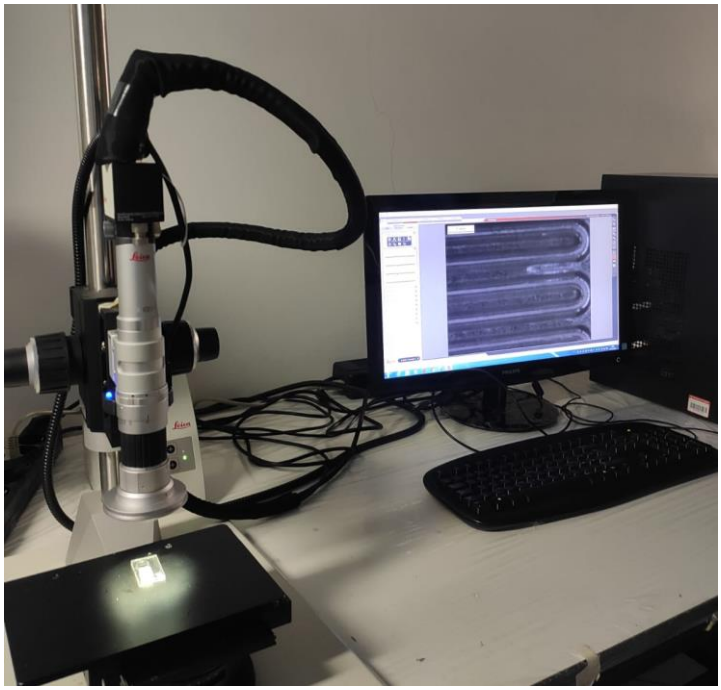

Figure 4.8 - Chilab Leica digital microscope

4.3.2 Field Emission Scanning Electron Microscope (FESEM)

The FESEM shown in the Figure 4.9[95] was used to perform a compositional analysis of the spinned and fiber-coated silicon substrate and also to analyze the fiber morphology of PAN. The field emission scanning electron microscope or FESEM is a microscope that involves the use of electrons. The source of the electrons is a cold tungsten needle that generates a high electric field gradient. These primary electrons are focused and deflected by electron lenses within the high vacuum column to produce a beam that bombards the samples, thereby emitting a beam of secondary electrons. The velocity and angle of these secondary electrons indicate the surface structure of the samples. A detector captures the secondary electrons and makes an electronic signal that is amplified and transformed into a digital image.

Figure 4.9 – ZEISS MERLIN FE-SEM[95]

4.4 Nanofibers inclusion

One of the most complex steps was to find the right technology that would allow us to integrate the nanofibers inside the microfluidic channels, ensuring a good resistance of the NFs layer to the passage of fluids. In this regard, the substrate chosen for the deposition of the polyacrylonitrile nanofibers was silicon because of a number of advantages encountered in the final objective, among them the fact that silicon conducts very well thermally and has a very low thickness. Tests were also carried out on a glass substrate, which for its part also has a number of properties that could lend themselves well, in particular its transparency that provides a high inspection capability at the technological level. The problem is that glass is more fragile than silicon and has an insulating effect, limitations that were not compatible with the technologies used in the next steps.

The following will explain the various steps that allowed to obtain this functionalization of the substrate, to get to the final step of assembling the internal device with the appropriate bonding technique.

4.4.1 Substrate preparation

To enable good deposition of the nanofibers on the silicon substrate, it was chosen to coat the substrate itself with PDMS. The natural ability of PDMS to be sticky exposes it to a very wide range of materials, including polymeric nanofibers, in our case PAN-based, favoring a better adhesion of the nanofibers. The coating of the substrate was realized by spin coating, a procedure that precisely allows to realize a thin and uniform film of about 10 mm. The silicon wafer was previously cut along preferred crystallographic directions to obtain a portions. Basically, a diamond bit was used to nick an edge of the wafer and pressure was applied at the same point, using a scalpel, for the crack to propagate along the wafer. Subsequently, a drop of silicone mixture was deposited in the center of the substrate, which was placed on the spin-coater to start the rapid rotation. The process was optimized and the various parameters are shown in *Table 4.1*

Spincot	RPM/time	Acc.RPM/sec
10	4000 rpm/60sec	1000

Table 4.1- spin coating parameters

Upon complete spin-coater shutdown, the substrate was placed on a plate at a temperature of 95°C for a time of 15 minutes to allow for complete cross-linking of the PDMS layer.

4.4.2 Inclusion and patterning of NFs in the concentration area

After preparing the substrate, deposition of PAN nanofibers was carried out by electrospinning technique (MECC NANON 01A) (Figure 4.10). The electrospinning is the unique technique that guarantees the formation of nanofibers' mat, characterized by a diameter distribution in the range between some nanometers to few micrometers. One of the main advantages of this process is focused on the possibility to collect the nanofibers directly onto the substrate of interest. In this thesis project, the first substrate is based on

Silicon covered by a PDMS layer. The sample was placed inside the machine onto the counter electrode, after loading the syringe with the polymeric solution, containing Polyacrylonitrile (PAN, Mw=120kDa, purchased from Sigma-Aldrich) dissolved into a proper solvent N-N Dimethylformamide (N-N DMF, purchased from Sigma Aldric). The electrospinning process is performed by applying a potential between two electrodes, the first one is defined spinneret, where the syringe is places, and the second one is defined counter electrode where the substrate is positioned, and its potential is equal to ground potential. The voltage applied is equal to 12 kV and time process is close to 30 min. Time process strictly affect the thickness of the final nanofibers' mats. In this context, several trials were performed, with different process lengths, which allowed us to test different thicknesses of the nanofiber layer. The reason for these tests was related to the fact that different thicknesses provided different results in the next step of patterning of the fibers themselves. In particular it was possible to demonstrate how thin thicknesses did not allow a proper removal but caused damage to the underlying PMDS layer.

Figure 4.10 - Chilab electrospinner MECC NANON-01 A

The next step was to reproduce the geometry of the microfluidics on the nanofibers that were patterned by the laser ablation technique, using the CO_2 laser of the LASER Slider Marker System (Figure 4.11). LASER Slider is a marker model consisting of:

- laser system with a CO_2 source working at 25-50W power
- galvanometric head used to guide the laser beam towards the samples
- cursor used to position the samples

- integrated computer used to load the CAD and adjust the process parameters.

Figure 4.11 – LASER Slider Marker System by Microla

In order to achieve proper nanofiber removal without damaging the underlying PDMS layer and causing carbonization of the PAN, different combinations of laser parameters were tested, among them different scan speeds and different powers. The test parameters were summarized in table *Table 4.2*

Test	Line	Line spacing [mm]	Angle	Steps	Power	Frequency [Hz]	V_p [mm/s]
P1	Crisscross	0,03	45°	1	20%	2000	800
P2	Crisscross	0,03	45°	1	20%	2000	600
P3	Crisscross	0,03	45°	1	20%	2000	400
P4	Crisscross	0,03	45°	1	10%	2000	150
P5	Crisscross	0,03	45°	1	10%	2000	50
P6	Crisscross	0,03	45°	1	5%	2000	500
P7	Crisscross	0,03	45°	1	5%	2000	100

Table 4.2 - Laser ablation conditions.

The parameters that most affected the results were scanning speed and laser power: high powers produced carbonization of the fibers and the underlying PDMS and associated with high speeds did not reproduce the exact geometry of the microfluidics.

4.5 Device sealing procedure

In order to obtain the complete device, the final step was to find the right bonding technique, which would allow to integrate the PDMS microfluidic chip with the nanofiber pattern, so that a specific volume of sample could be confined inside the channels and everything could stand up to subsequent leak tests. This was the most complex step, in which several methods were tested, among them: plasma bonding and plasma etching. Both, however, did not allow us to obtain the desired results.

The first bonding tests have been carried out using oxygen plasma treatments (Electronic Diener Plasma-Surface-Technology) (Figure 4.12) to increase the surface energy and make the device ready for bonding. PDMS comprises repeated units of— $O—Si(CH_3)_2—$, which upon exposure to oxygen plasma develops silylene (-OH) and loses methyl groups ($—CH_3$). These silylanolic groups, being strongly polar groups, make the surface hydrophilic and condensing with those present on another PDMS surface produces Si-O-Si bonds with loss of a water molecule, thus promoting the formation of a strong covalent bond between the two layers.

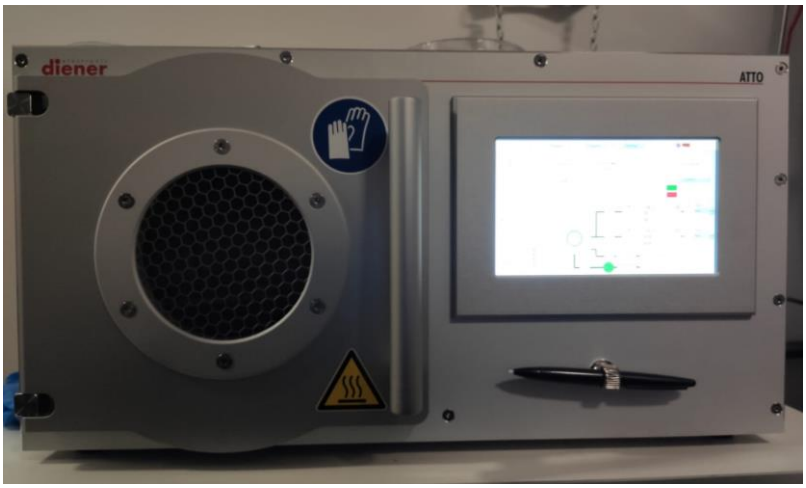

Figure 4.12 - Chilab Plasma Diener Electronic Reactor

Before treatment, the PDMS chip was cleaned in the ultrasonic bath with 2-propanol for 1 min and then dried for 1 min with nitrogen flow. The silicon substrate with the patterned nanofibers was placed in the plasma system together with the samples and they were exposed to the treatment. The process is divided into five phases: in the first phase, called the pumping down period, the pressure in the chamber drops to 0.3 mbar. In the second step, oxygen is insufflated into the chamber with the samples with a pressure of 0.70 mbar for one minute, after which the high frequency generator is activated and plasma takes place for 30 seconds with a power of 22%. The last step is venting where the chamber is filled with air. After surface treatment, the system was assembled to align the microfluidic channels

with the patterned fibers by exerting gentle finger pressure for 5 seconds to promote bonding. The main problem of this treatment was related to the imperfect removal of the nanofibers by laser ablation, which did not allow the exposure of the underlying PDMS compromising the tightness of the device, because a good PDMS-PDMS bond was not guaranteed and therefore the device detached very easily from the substrate.

Another technique that has been tested in an attempt to optimally remove the fibers and thus promote good bonding is plasma etching, a technique that consists of an attack on the surface by means of a reactive process gas (oxygen) that allows the removal of material in the gas phase which is then expelled by the vacuum pump. However, this technique proved to be unsuitable for this case, because by testing electrospun but not patterned samples it was seen that even at very low process times (5 minutes) cracks were produced in the underlying PDMS and this did not guarantee a good seal. The tests were carried out with Plasmafab 508.

5. Results and discussion

The following are the results obtained as a result of sample characterizations performed by digital microscope and field emission scanning electron microscope (FESEM) to investigate physical characteristics such as dimensions and surfaces, the results obtained from seal tests to evaluate the effectiveness of the chosen bonding technique, and the results from digital microscope characterizations to evaluate the state of the fibers after the passage of the test fluids.

5.1 Mold characterization

Based on the starting measurements from the CAD model, where each channel has a 500 µm x 500 µm square cross section with a 500 µm space separating them from each other, we went to evaluate how well the replica molding process would allow us to reproduce these measurements. Below are the characterizations that were made under a digital microscope (Figure 5.2), along with the corresponding measurements made on a central portion of the channels of a PDMS replica (Figure 5.1).

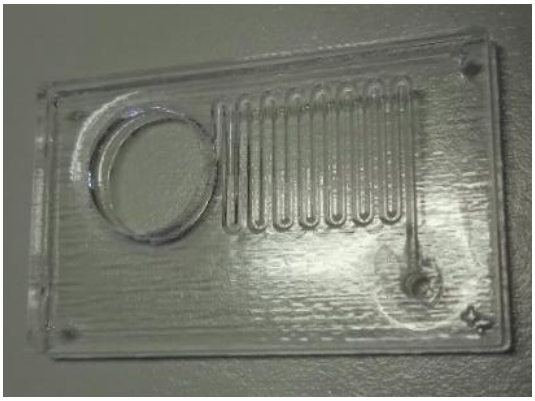

Figure 5.1 – Replica molding

Specifically, the measurements were performed on a section of the replica, on which a cut was made with the help of a razor blade that allowed us to obtain the two halves of the chip and then from these we obtained the analyzed portion.

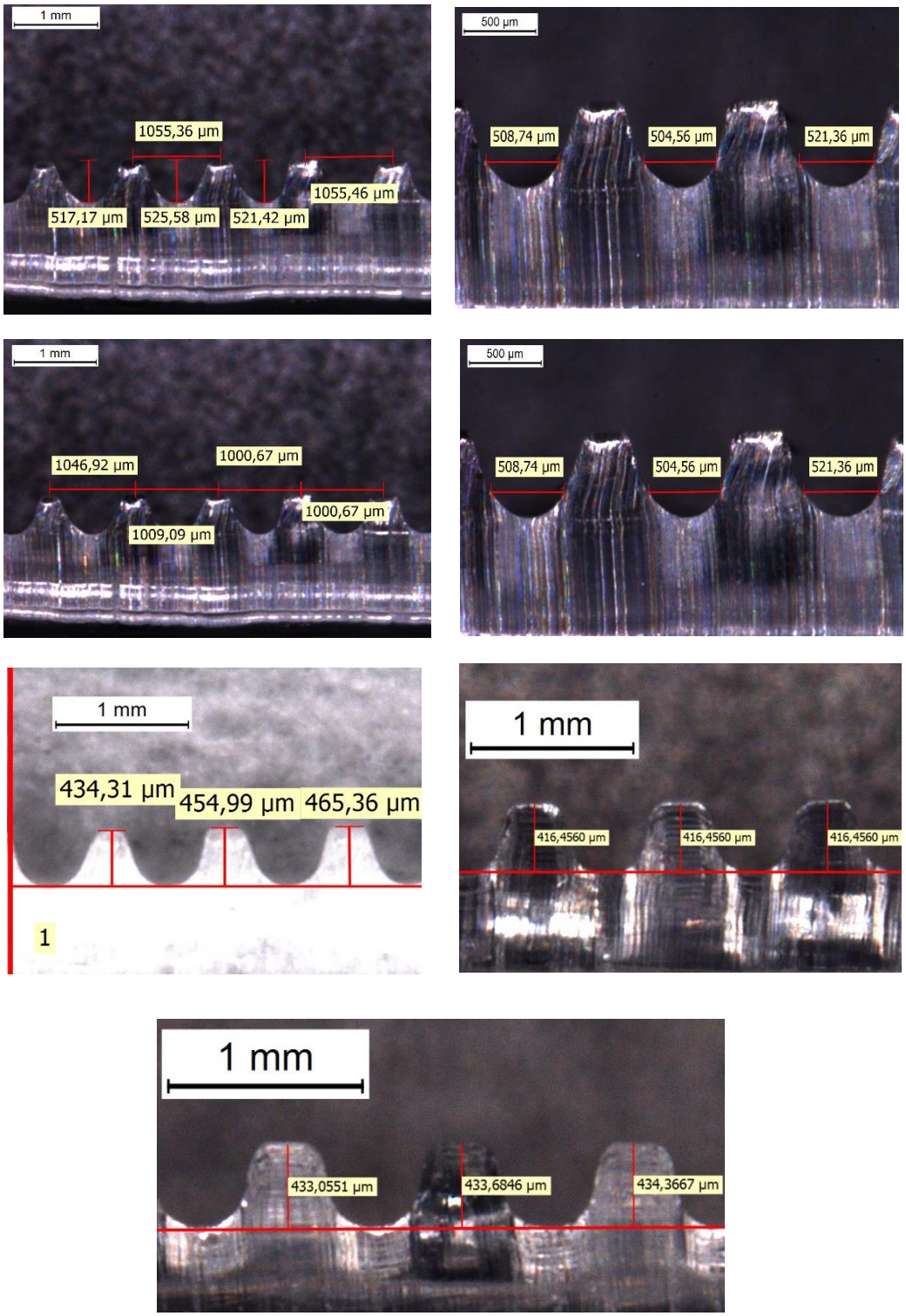

Figure 5.2 - Sectional view of the microfluidic channels of four PDMS replicas, with related measurements of heights and distances

On the basis of the characterizations we carried out, it was possible to observe that the heights of the channels vary in a rather narrow range compared to that predicted by the CAD model and therefore allowed us to achieve good results in the following steps.

5.2 Field Emission Scanning Electron Microscope (FESEM)

The purpose was to perform an analysis by energy dispersive spectrometry (EDS) in order to evaluate the effect of laser ablation on the nanofibers and its capability to complete remove PAN nanofibers. Figure 5.3 reports the images of a sample analyzed after laser ablation with the respective compositional result. EDS results allowed highlighting the presence of oxygen (O), carbon (C), nitrogen (N) and silicon (Si), of which the energy peaks are represented. From the percentages by weight we can see that the area of interest, squared, has a certain percentage of all the elements: Si is present in a percentage by weight of 16.61% because the substrate we are analyzing is precisely a silicon substrate; carbon and oxygen, present at 53.36% and 9.16% respectively, can be found in PDMS and carbon also in PAN nanofibers; nitrogen instead, present at 20.88% by weight, is a material that can be present only in PAN and not in PDMS. In particular, the presence of nitrogen leads to demonstrate how the laser ablation did not perform a complete removal of PAN nanofibers, which lost the nanostructuration and a film was formed.

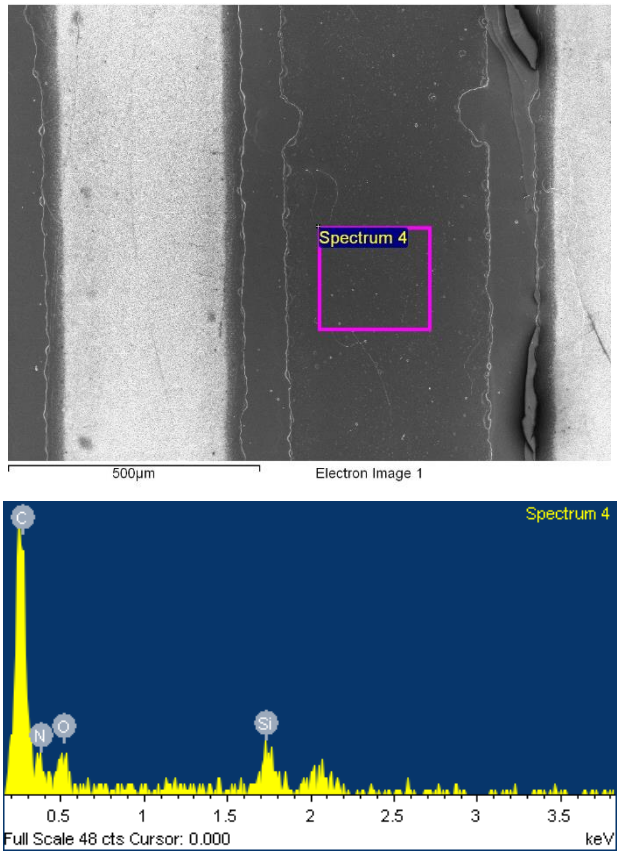

Figure 5.3 - In the first image we see the area analyzed by FESEM, in the second image the EDS spectrum that shows us the energy peaks of the elements present in the sample analyzed.

On the same sample, another portion was also analyzed and EDS analysis was performed Figure 5.4. Here different weight percentages of the different materials were found: there is a higher percentage by weight of silicon (43.02%) always related to the fact that the substrate analyzed is silicon-based; oxygen and carbon present respectively at 26.76% and 30.21%, can be associated with both the presence of PDMS and PAN, but in this case there is a zero weight percentage of nitrogen, a component that can be recorded only in PAN fibers and not in PDMS. From this analysis, therefore, it could be observed that with laser ablation the fibers can be correctly removed only at the edges of the channels, while throughout the central film analyzed in Figure 5.3 there is a certain amount of PAN present. This is related to the fact that the laser, when the process is started, first engraves the central area of the pattern and at the end engraves the perimeter, then runs through the area near the edges twice and this allows it to remove the fibers.

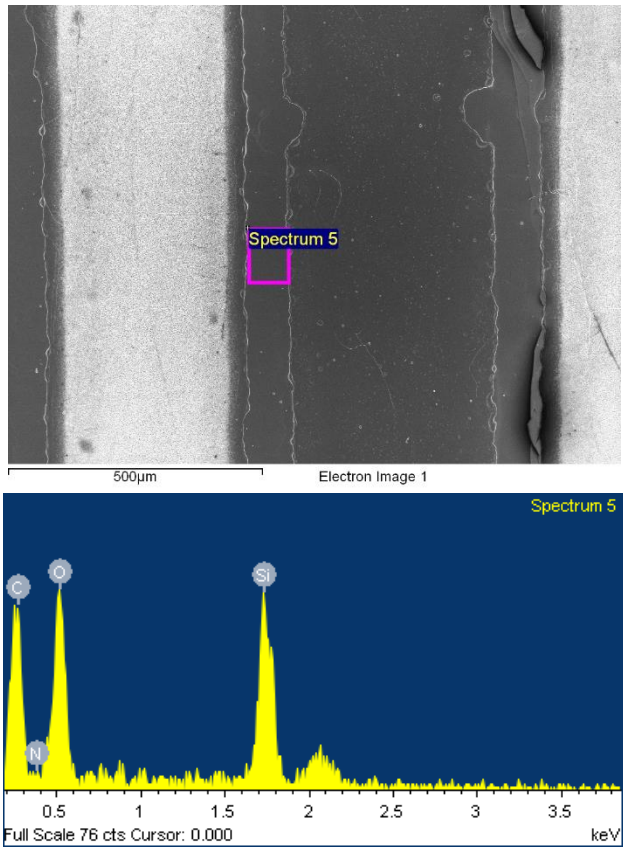

Figure 5.4 - In the first image we see the area analyzed by FESEM, in the second image the EDS spectrum that shows us the energy peaks of the elements present in the sample analyzed.

From this analysis we found the way to obtain a correct ablation of the fibers not only at the edge of the channels but throughout the space that separates the channels themselves, going to increase the diameter of the fibers from 500 µm to 900 µm, so that at the second pass of the laser when it goes to cut the perimeter these are removed.

On the other hand, regarding the morphological characterization of the electrospinned nanofibers, the images that were captured are shown in Figure 5.5.

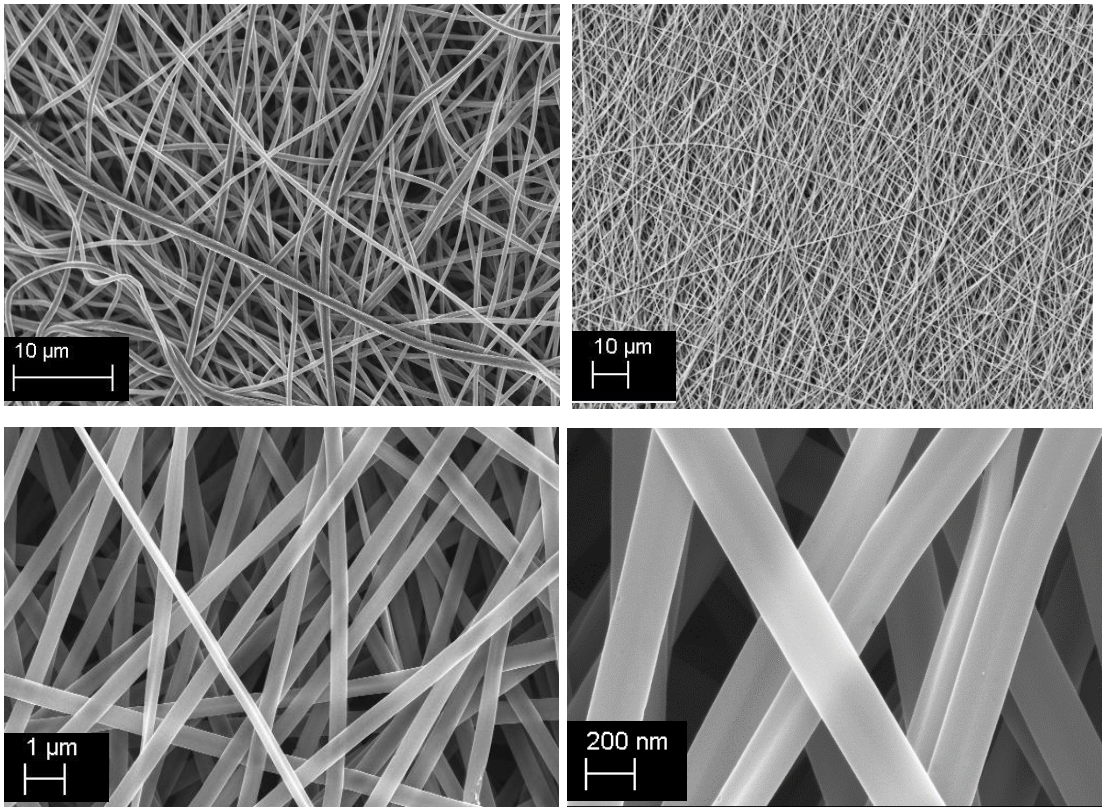

Figure 5.5 – Morphological characterization of PAN nanofibers at different magnification

The Fesem images represent the morphological properties of the nanofibers: it was possible to appreciate the high surface/volume ratio guaranteed by the nanofiber distribution, the high porosity ensured and the absence of defects. All these intrinsic properties may be suitable for this nanostructuring to improve and increase the surface available for functionalization thus leading to improve the final performance of the device.

5.3 Patterning of nanofibers and final assembly of the microfluidic system

As previously explained, the laser parameters were optimized in order to achieve a correct ablation of the nanofibers avoiding carbonization issues, which strongly affect the final assembly of the microfluidic system. The nanofibers around the microfluidics were also removed, in order to ensure optimal bonding with the microchip. The final parameters that allowed us to achieve the goal are shown in the table 5.1.

Line	Line spacing [mm]	Angle	Steps	Power	Frequency [Hz]	Vs [mm/s]
Crisscross	0,03	45°	1	2%	2000	70

Table 5.1 - Laser parameters

The pattern obtained with the above parameters is shown in *Figure 5.6*

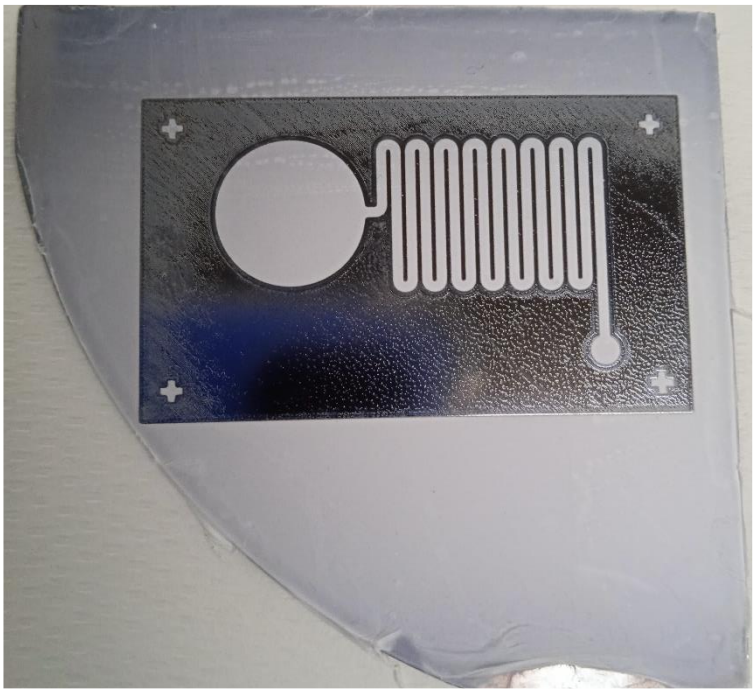

Figure 5.6 - Nanofibers patterned by laser ablation

Final step in the fabrication of the microfluidic device is the one related to the bonding process. The selected technique, which allowed us to achieve a stable assembly of the whole device, is the interlayer bonding technique, which involved the use of a thin layer of non-crosslinked PDMS. The technique involved the following steps:

- uniform application of a thin layer of PDMS on a PMMA substrate

- Placement of the microfluidic chip on this layer in order to transfer a part of it on the surface to be bonded.
- transfer of the chip on a plate (at 70°C for 10 minutes) to allow a partial crosslinking of the PDMS thin layer and to avoid that it enters inside the channels during the closing phase
- final assembly with the silicon wafer covered by the patterned fibers
- curing in oven at 95°C for 45 minutes.

The described technique allowed us to obtain the final device that is shown in *Figure 5.7*

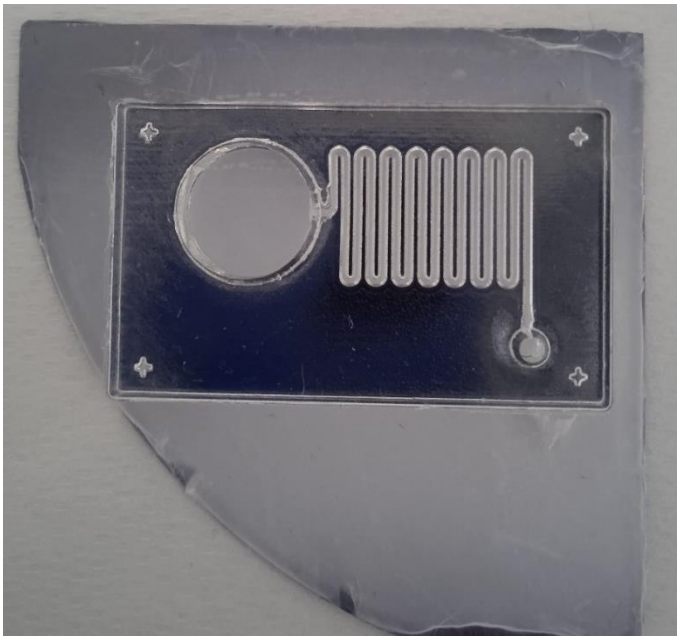

Figure 5.7 - Assembled microfluidic system: the chip has been bonded by interlayer bonding technique, ensuring a good alignment of the channels with respect to the patterned nanofibers

5.4 Leack test

Once the complete device was obtained, leak tests were performed to observe whether the assembly between the PDMS chip and the substrate with the patterned nanofibers held up and whether there were no leaks as test fluids passed through. 40 µl of solution of blue dye and deionized water was prepared in a 1:3 (v/v) ratio and was injected using a syringe attached to a 1.5 mm tube so that the solution would flow within the microfluidic channels, filling the concentration area. What we wanted to achieve was no leakage and confinement

of the fluid within the channels. The results of leak tests performed on 3 samples are shown in Figure 5.8.

Figure 5.8 – Images of leak test on 3 different sample

Another protocol tested to assess the tightness of the microfluidic device was the injection of ethanol with subsequent closure of the inlet and outlet of the device with parafilm to prevent evaporation of the liquid in oven at 60°C for 10 minutes (Figure 5.9).

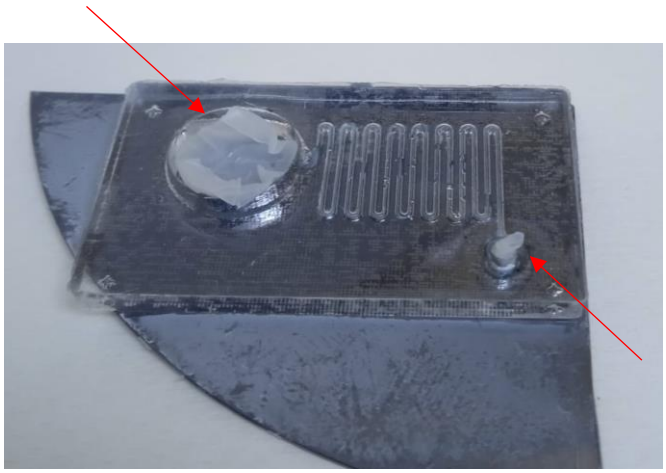

Figure 5.9 - Device subjected to the ethanol leak test; those indicated with red arrows represent the inlet and outlet areas closed with parafilm.

Images of the ethanol leak test results are shown in (Figure 5.10): small bubbles were observed inside the channels during ethanol evaporation, but no detachment of the device occurred.

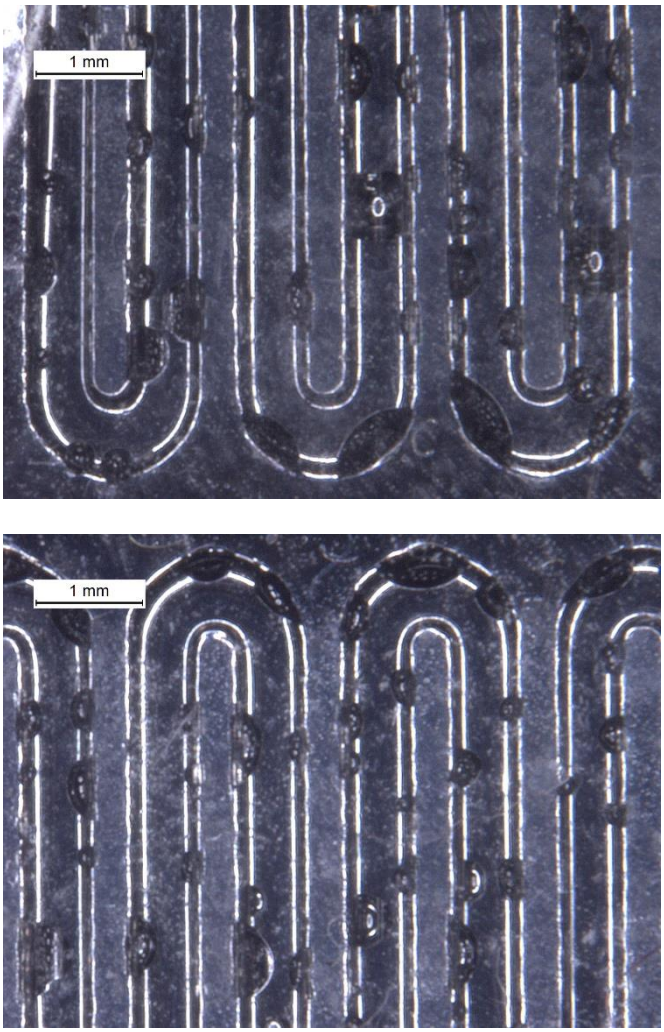

Figure 5.10 - Digital microscope images of microfluidic channels after ethanol leak test

5.5 Nanofibers characterization

After the tightness tests, the state of the nanofibers after the passage of the fluid was studied. In this regard, some samples were taken from the silicon substrate with the aid of a spatula to detach the PDMS layer used for bonding, paying attention not to remove the nanofibers. Once the chip was removed, the state of the fibers was analyzed under a digital microscope (Leica81). It was found that the fibers maintained their initial morphology, even after being subjected to the flow of test fluids (Figure 5.11).

There were areas where, however, the nanofibers seem a little damaged and crumpled, this effect it is precisely due to the removal of the chip from the substrate, as the PDMS layer used to bond once cross-linked tends to guarantee a very stable seal with the substrate and therefore "forcing" the removal this slight lifting has occurred of nanofibers. However, we can say that we have achieved the desired result: the nanofibers remained well aligned in the channels.

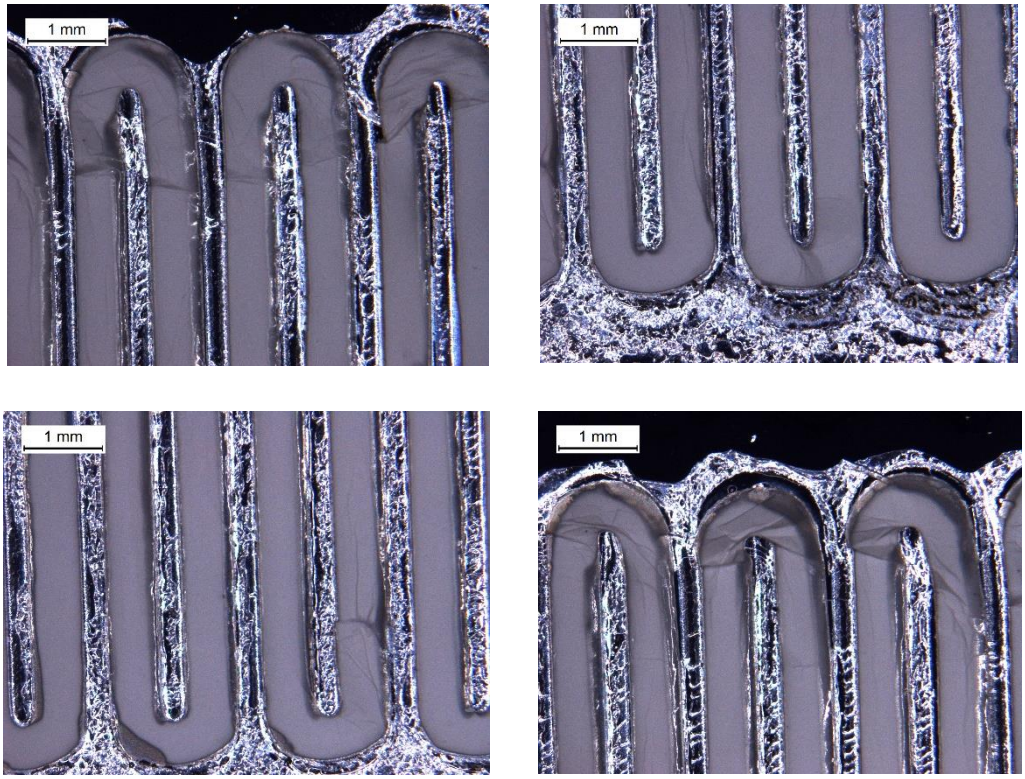

Figure 5.11 - Digital microscope images of nanofiber morphology after the leak test, relative to 4 different samples

6. Conclusion and future work

In this thesis work, a microfluidic Lab-on-a-Chip has been realized with polyacrylonitrile (PAN) based nanofibers, directly integrated within the microfluidic channels, which thanks to their surface chemistry characterized by the presence of amino groups, which can be activated through subsequent plasma treatments, are able to facilitate the capture of miRNAs.

In this regard, a fabrication approach was defined that could combine optimized chip bonding and nanofiber patterning ensuring good resistance of the nanofiber layer during fluid flow at different speeds in the microfluidic system, without inducing damage or detachment of the matte nanofibers.

The starting point was a chip layout designed using a 2D model from Rhinoceros software (Robert McNeel & Associates), followed by a 3D STL model prepared with the same CAD. The device, with dimensions 10.5 mm x 15.5 mm, is composed of a well in which the biological sample is inserted, an outlet where all the waste is aspirated and a concentration zone, represented by microfluidic channels (500 µm x 500 µm square section).

The design phase was followed by the realization phase of the device: the technique used in this regard is that of replica molding, which involved the use of a poly-jet 3D printer (OBJET 30 by Stratasys) to manufacture the master mold, which in turn was used to obtain PDMS replicas of the microfluidic system. Once the replicas were obtained, a characterization of the PDMS chips was performed under a digital microscope in order to evaluate the dimensions of the channels and how close they were to those thought in the design phase.

The next step was the inclusion of electrospun PAN nanofibers that were deposited directly onto a silicon substrate covered by a layer of PDMS, previously spin coated onto it.

In order to pattern the nanofibers with the same geometry as the microfluidic device, the laser ablation technique was exploited using a custom laser cutting machine. In order to achieve optimal pattern transfer, without damaging the nanofibers or the underlying PDMS layer, the laser parameters were optimized and the following were used in the final tests: 2% power, 2000 Hz frequency and 70 mm/s scanning speed.

To obtain the final assembled device, a number of bonding techniques were tested and the one that achieved optimal bonding was interlayer bonding: a thin layer of uncured PDMS was spread on the microfluidic chip that allowed bonding on the silicon wafer. This was first placed on a plate to allow partial crosslinking of the PDMS layer and then in an oven to complete polymerization.

In order to test the tightness of the final device, two tests were performed: injection of a dye by syringe to observe the flow of liquid inside the channels; injection of ethanol, again by

syringe, with subsequent closure of the inlet and outlet of the device with parafilm to prevent evaporation of the liquid in the oven (at 60 °C for 10 minutes) to verify the effective tightness of the bonding without detachment. From these leak tests it was observed that the injected test fluids remained well confined within the microfluidic channels, no detachments were produced during the evaporation phase of ethanol, but above all, through microscopic characterizations it was found that the fibers, despite the passage of fluids, maintained the morphology of departure.

In conclusion, the successfully designed, fabricated and tested LOC was conceived with a view to make more efficient, easier, faster, low energy and low cost process of concentration and subsequent amplification of viral RNA using an isothermal amplification method.

In this regard, for the implementation of subsequent biological experiments, it is already suggested the modification to be made to the CAD of the device that improves those aspects that may not be suitable for the biological protocols to be followed: the size of the inlet well into which the biological sample is to be loaded has been reduced and the size of the microfluidic channels has been reduced from a square section of 500 µm x 500 µm to one of 500 µm x 250 µm in order to reduce the volume of fluids to be injected (from 41 µl to 10 µl).

Bibliography

1. Valentine, R. C. Virus structure. *Sci. Basis Med. Annu. Rev.* 256–266 (1969) doi:10.1016/b978-0-12-803109-4.00002-7.
2. It, E. & Your, W. Viruses Definition : A Case Study Guide About Life of Viruses.
3. Covid-, C. "CORONAVIRUS CoViD-19". (2020).
4. Payne, S. Introduction to RNA Viruses. *Viruses* 97–105 (2017) doi:10.1016/b978-0-12-803109-4.00010-6.
5. Microbiologia Italia. https://www.microbiologiaitalia.it/virologia/virus/.
6. Philipson, L. *Replication, transcription and translation of RNA viruses*. *Textbook of Medical Virology* (Butterworth & Co. (Publishers) Ltd, 1983). doi:10.1016/b978-0-407-00253-1.50013-x.
7. Basova, E., Neu, P., Zhu, H., Fohlerov, Z. & Pek, J. Biosensors and Bioelectronics Recent advances in lab-on-a-chip technologies for viral diagnosis. **153**, (2020).
8. Tomlinson, J. A., Dickinson, M. J. & Boonham, N. Rapid detection of phytophthora ramorum and P. kernoviae by two-minute DNA extraction followed by isothermal amplification and amplicon detection by generic lateral flow device. *Phytopathology* **100**, 143–149 (2010).
9. Mullis, K. B. The unusual origin of the polymerase chain reaction. *Sci. Am.* **262**, 56–65 (1990).
10. Jalali, M., Zaborowska, J. & Jalali, M. *The Polymerase Chain Reaction: PCR, qPCR, and RT-PCR*. *Basic Science Methods for Clinical Researchers* (Elsevier Inc., 2017). doi:10.1016/B978-0-12-803077-6.00001-1.
11. Fredricks, D. N. & Relman, D. A. Application of polymerase chain reaction to the diagnosis of infectious diseases. *Clin. Infect. Dis.* **29**, 475–488 (1999).
12. Daniel H. Farkas, C. A. H. Overview of Molecular Diagnostic Techniques and Instrumentation. in.
13. Yang, S. & Rothman, R. E. PCR-based diagnostics for infectious diseases: Uses, limitations, and future applications in acute-care settings. *Lancet Infectious Diseases* vol. 4 337–348 (2004).
14. Vaneechoutte, M. & Van Eldere, J. The possibilities and limitations of nucleic acid amplification technology in diagnostic microbiology. *J. Med. Microbiol.* **46**,

188–194 (1997).

15. Francois, P. *et al.* Robustness of a loop-mediated isothermal amplification reaction for diagnostic applications. doi:10.1111/j.1574-695X.2011.00785.x.
16. Parida, M., Posadas, G., Inoue, S., Hasebe, F. & Morita, K. Real-time reverse transcription loop-mediated isothermal amplification for rapid detection of West Nile virus. *J. Clin. Microbiol.* **42**, 257–63 (2004).
17. Notomi, T. *et al.* Loop-mediated isothermal amplification of DNA. *Nucleic Acids Res.* **28**, 63e – 63 (2000).
18. Nagamine, K., Hase, T. & Notomi, T. Accelerated reaction by loop-mediated isothermal amplification using loop primers. *Mol. Cell. Probes* **16**, 223–229 (2002).
19. Alhassan, A., Li, Z., Poole, C. B. & Carlow, C. K. S. Expanding the MDx toolbox for filarial diagnosis and surveillance. *Trends in Parasitology* vol. 31 391–400 (2015).
20. Curtis, K. A., Niedzwiedz, P. L., Youngpairoj, A. S., Rudolph, D. L. & Owen, S. M. Real-Time Detection of HIV-2 by Reverse Transcription–Loop-Mediated Isothermal Amplification. *J. Clin. Microbiol.* **52**, 2674–2676 (2014).
21. Liu, J. *et al. Development of reverse-transcription loop-mediated isothermal amplification assay for rapid detection of novel avian influenza A (H7N9) virus*. http://www.biomedcentral.com/1471-2180/14/271 (2014) doi:10.1186/s12866-014-0271-x.
22. Koczula, K. M. & Gallotta, A. Lateral flow assays. *Essays Biochem.* **60**, 111–120 (2016).
23. Boisen, M. L. *et al.* Development of Prototype Filovirus Recombinant Antigen Immunoassays. *J. Infect. Dis.* **212**, S359–S367 (2015).
24. Koczula, K. M. & Gallotta, A. Lateral flow assays. 111–120 (2016) doi:10.1042/EBC20150012.
25. Fung, K. K., Chan, C. P. Y. & Renneberg, R. Development of enzyme-based bar code-style lateral-flow assay for hydrogen peroxide determination. *Anal. Chim. Acta* **634**, 89–95 (2009).
26. Engvall, E. & Perlmann, P. Enzyme-linked immunosorbent assay (ELISA) quantitative assay of immunoglobulin G. *Immunochemistry* **8**, 871–874 (1971).

27. Zhuang, J., Yin, J., Lv, S., Wang, B. & Mu, Y. Biosensors and Bioelectronics Advanced " lab-on-a-chip " to detect viruses – Current challenges and future perspectives. *Biosens. Bioelectron.* **163**, 112291 (2020).
28. Il testo. 107–186 (2012) doi:10.1484/m.tvma-eb.4.00154.
29. Lequin, R. M. Enzyme immunoassay (EIA)/enzyme-linked immunosorbent assay (ELISA). *Clin. Chem.* **51**, 2415–2418 (2005).
30. CD Creative Diagnostic. https://www.creative-diagnostics.com/ELISA-guide.htm.
31. Dobrovolskaia, E., Gam, A., Slater, J. E., Slater, J. E. & Hfm-, F. *Competition enzyme-linked immunosorbant assay (ELISA) can be a sensitive method for the specific detection of small quantities of allergen in a complex mixture*. http://www.inbio.com/protocols.html.
32. Lim, Y. C., Kouzani, A. Z. & Duan, W. Lab-on-a-chip: A component view. *Microsyst. Technol.* **16**, 1995–2015 (2010).
33. Nikoleli, G. P. *et al.* Biosensors based on microfluidic devices lab-on-a-chip and microfluidic technology. in *Nanotechnology and Biosensors* 375–394 (Elsevier, 2018). doi:10.1016/B978-0-12-813855-7.00013-1.
34. Dhar, B. C. & Lee, N. Y. Lab-on-a-Chip Technology for Environmental Monitoring of Microorganisms. *Biochip J.* **12**, 173–183 (2018).
35. Vikram Vemula, S. *et al.* viruses Current Approaches for Diagnosis of Influenza Virus Infections in Humans. doi:10.3390/v8040096.
36. Hay, A. J., Gregory, V., Douglas, A. R. & Yi, P. L. The evolution of human influenza viruses. *Philos. Trans. R. Soc. B Biol. Sci.* **356**, 1861–1870 (2001).
37. Wu, Y., Wu, Y., Tefsen, B., Shi, Y. & Gao, G. F. Bat-derived influenza-like viruses H17N10 and H18N11. *Trends in Microbiology* vol. 22 183–191 (2014).
38. Boon, A. C. M., French, A. M. F., Fleming, D. M. & Zambon, M. C. *Detection of In¯uenza A Subtypes in Community-Based Surveillance*. *Journal of Medical Virology* vol. 65 (2001).
39. Dzi, K., Abowska, ¸, Zbieta Czaczyk, E. & Nidzworski, D. Detection Methods of Human and Animal Influenza Virus-Current Trends. doi:10.3390/bios8040094.
40. Simple, A. A Simple, Cost-Effective Undergraduate Workshop Based on Simulated Complement Fixation Test to Teach the Concept of Complement

System. *Eur. J. Heal. Biol. Educ.* **8**, 19–30 (2019).

41. Ellis, J. S. & Zambon, M. C. Molecular diagnosis of influenza. *Rev. Med. Virol.* **12**, 375–389 (2002).
42. Ravina, Dalal, A., Mohan, H., Prasad, M. & Pundir, C. S. Detection methods for influenza A H1N1 virus with special reference to biosensors: A review. *Biosci. Rep.* **40**, 1–18 (2020).
43. Tseng, Y. T., Wang, C. H., Chang, C. P. & Lee, G. Bin. Integrated microfluidic system for rapid detection of influenza H1N1 virus using a sandwich-based aptamer assay. *Biosens. Bioelectron.* **82**, 105–111 (2016).
44. Ma, Y. D., Chen, Y. S. & Lee, G. Bin. An integrated self-driven microfluidic device for rapid detection of the influenza A (H1N1) virus by reverse transcription loop-mediated isothermal amplification. *Sensors Actuators, B Chem.* **296**, 126647 (2019).
45. Shen, K. M. *et al.* An integrated microfluidic system for rapid detection and multiple subtyping of influenza A viruses by using glycan-coated magnetic beads and RT-PCR. *Lab Chip* **19**, 1277–1286 (2019).
46. Longo, D. L., Musso, D., Ko, A. I. & Baud, D. Zika Virus Infection-After the Pandemic. *N Engl J Med* **381**, 1444–57 (2019).
47. Baud, D., Gubler, D. J., Schaub, B., Lanteri, M. C. & Musso, D. An update on Zika virus infection. *The Lancet* vol. 390 2099–2109 (2017).
48. Blaes, F. Pathogenesis, diagnosis and treatment of paraneoplastic neurologic syndromes. *Expert Rev. Neurother.* 14737175.2021.1927713 (2021) doi:10.1080/14737175.2021.1927713.
49. Jefferson, S., Da Silva, R., Pardee, K. & Pena, L. Loop-Mediated Isothermal Amplification (LAMP) for the Diagnosis of Zika Virus: A Review. (2019) doi:10.3390/v12010019.
50. Ganguli, A. *et al.* Hands-free smartphone-based diagnostics for simultaneous detection of Zika, Chikungunya, and Dengue at point-of-care. doi:10.1007/s10544-017-0209-9.
51. Yang, B., Kong, J. & Fang, X. Bandage-like wearable flexible microfluidic recombinase polymerase amplification sensor for the rapid visual detection of nucleic acids. *Talanta* **204**, 685–692 (2019).

52. PDMS SYLGARD. https://www.sigmaaldrich.com/catalog/product/aldrich/761036?lang=it&region=IT&gclid=EAIaIQobChMIoLWYhq7V8AIVh5eyCh00xA-9EAAYASAAEgIhUfD_BwE.

53. Potrich, C. *et al.* Simple PDMS microdevice for biomedical applications. *Talanta* **193**, 44–50 (2019).

54. Rezaei, Z. & Mahmoudifard, M. Pivotal role of electrospun nanofibers in microfluidic diagnostic systems-a review. *J. Mater. Chem. B* **7**, 4602–4619 (2019).

55. Sanjay, S. T., Dou, M., Sun, J. & Li, X. A paper/polymer hybrid microfluidic microplate for rapid quantitative detection of multiple disease biomarkers OPEN. *Nat. Publ. Gr.* (2016) doi:10.1038/srep30474.

56. Jung, W., Han, J., Choi, J. W. & Ahn, C. H. Point-of-care testing (POCT) diagnostic systems using microfluidic lab-on-a-chip technologies. *Microelectronic Engineering* vol. 132 46–57 (2015).

57. Oliveira, O. N., Iost, R. M., Siqueira, J. J., Crespilho, F. N. & Caseli, L. Nanomaterials for Diagnosis: Challenges and Applications in Smart Devices Based on Molecular Recognition. (2014) doi:10.1021/am5015056.

58. Carrascosa, L. G., Moreno, M., Álvarez, M. & Lechuga, L. M. Nanomechanical biosensors: A new sensing tool. *TrAC - Trends Anal. Chem.* **25**, 196–206 (2006).

59. Ding, B., Wang, M., Wang, X., Yu, J. & Sun, G. Electrospun nanomaterials for ultrasensitive sensors. *Mater. Today* **13**, 16–27 (2010).

60. Wallin, P. *et al.* A method to integrate patterned electrospun fibers with microfluidic systems to generate complex microenvironments for cell culture applications. doi:10.1063/1.4729747.

61. Ren, K., Zhou, J. & Wu, H. Materials for Microfluidic Chip Fabrication. (2001) doi:10.1021/ar300314s.

62. Fujii, T. *PDMS-based microfluidic devices for biomedical applications*. www.elsevier.com/locate/mee (2002).

63. Carrell, C. S., McCord, C. P., Wydallis, R. M. & Henry, C. S. Sealing 3D-printed parts to poly(dimethylsiloxane) for simple fabrication of Microfluidic devices. *Anal. Chim. Acta* **1124**, 78–84 (2020).

64. Cabeza, V. S. High and Efficient Production of Nanomaterials by Microfluidic Reactor Approaches. *Adv. Microfluid. - New Appl. Biol. Energy, Mater. Sci.* (2016) doi:10.5772/64347.

65. Becker, H. & Gärtner, C. Polymer microfabrication technologies for microfluidic systems. doi:10.1007/s00216-007-1692-2.

66. Abgrall, P. & Gué, A.-M. Lab-on-chip technologies: making a microfluidic network and coupling it into a complete microsystem—a review. *J. Micromechanics Microengineering* **17**, R15–R49 (2007).

67. Yu, X.-Y. *Advances in Microfluidics - New Applications in Biology, Energy, and Materials Sciences*. (2016).

68. Henniker Scientific. PDMS. https://www.azom.com/article.aspx?ArticleID=14346.

69. PDMS: a review. Introduction to poly-di-methyl-syloxane (PDMS). https://www.elveflow.com/microfluidic-reviews/general-microfluidics/the-poly-di-methyl-siloxane-pdms-and-microfluidics-2/.

70. Vis-, A. Fibers : Acrylic. 1–13 (2006).

71. Mei, Y., Yao, C., Fan, K. & Li, X. Surface modification of polyacrylonitrile nanofibrous membranes with superior antibacterial and easy-cleaning properties through hydrophilic flexible spacers. *J. Memb. Sci.* **417–418**, 20–27 (2012).

72. Chimichiamo. Poliacrilonitrile. https://www.chimicamo.org/chimica-organica/poliacrilonitrile/.

73. Rainelli, A., Stratz, R., Schweizer, K. & Hauser, P. C. Miniature flow-injection analysis manifold created by micromilling. *Talanta* **61**, 659–665 (2003).

74. Han, A. & Li, J. Lab on a Chip Featuring work from the groups of Professor Title: Multi-compartment neuron-glia co-culture platform for localized CNS axon-glia interaction study. *Number* **12**, 3199–3522 (2012).

75. Andersson, H. & Van den Berg, A. Microfluidic devices for cellomics: A review. *Sensors Actuators, B Chem.* **92**, 315–325 (2003).

76. Qin, D., Xia, Y. & Whitesides, G. M. Soft lithography for micro- and nanoscale patterning. (2010) doi:10.1038/nprot.2009.234.

77. Kane, R. S., Takayama, S., Ostuni, E., Ingber, D. E. & Whitesides, G. M.

Patterning proteins and cells using soft lithography. *Biomaterials* **20**, 2363–2376 (1999).

78. Shih, T. K., Chen, C. F., Ho, J. R. & Chuang, F. T. Fabrication of PDMS (polydimethylsiloxane) microlens and diffuser using replica molding. *Microelectron. Eng.* **83**, 2499–2503 (2006).
79. Becker, H. & Gärtner, C. Polymer microfabrication technologies for microfluidic systems. *Anal. Bioanal. Chem.* **390**, 89–111 (2008).
80. Oxolutia. Electrospinning. http://www.oxolutia.com/technology/%0Aelectrospinning/.
81. Doshi, J. & Reneker, D. H. Electrospinning process and applications of electrospun fibers. *J. Electrostat.* **35**, 151–160 (1995).
82. Sun, B. *et al.* Advances in three-dimensional nanofibrous macrostructures via electrospinning. *Prog. Polym. Sci.* **39**, 862–890 (2014).
83. Ahmed, F. E., Lalia, B. S. & Hashaikeh, R. A review on electrospinning for membrane fabrication: Challenges and applications. *Desalination* **356**, 15–30 (2015).
84. Haider, A., Haider, S. & Kang, I. K. A comprehensive review summarizing the effect of electrospinning parameters and potential applications of nanofibers in biomedical and biotechnology. *Arabian Journal of Chemistry* vol. 11 1165–1188 (2018).
85. Bhardwaj, N. & Kundu, S. C. Electrospinning: A fascinating fiber fabrication technique. *Biotechnol. Adv.* **28**, 325–347 (2010).
86. Deitzel, J. M., Kleinmeyer, J., Harris, D. & Beck Tan, N. C. The effect of processing variables on the morphology of electrospun nanofibers and textiles. *Polymer (Guildf).* **42**, 261–272 (2001).
87. Beachley, V. & Wen, X. Effect of electrospinning parameters on the nanofiber diameter and length. *Mater. Sci. Eng. C* **29**, 663–668 (2009).
88. Fong, H., Chun, I. & Reneker, D. H. Beaded nanofibers formed during electrospinning. in *Polymer* vol. 40 4585–4592 (Elsevier Science Ltd, 1999).
89. Okutan, N., Terzi, P. & Altay, F. Affecting parameters on electrospinning process and characterization of electrospun gelatin nanofibers. *Food Hydrocoll.* **39**, 19–26 (2014).

90. Thenmozhi, S., Dharmaraj, N., Kadirvelu, K. & Kim, H. Y. Electrospun nanofibers: New generation materials for advanced applications. *Mater. Sci. Eng. B Solid-State Mater. Adv. Technol.* **217**, 36–48 (2017).
91. Zuo, W. *et al.* Experimental Study on Relationship Between Jet Instability and Formation of Beaded Fibers During Electrospinning. (2005) doi:10.1002/pen.20304.
92. Pelipenko, J., Kristl, J., Janković, B., Baumgartner, S. & Kocbek, P. The impact of relative humidity during electrospinning on the morphology and mechanical properties of nanofibers. *Int. J. Pharm.* **456**, 125–134 (2013).
93. Torino, P. D. I. & Lab-on-a-, F. E. Master ' s Degree Course in Electronic Engineering Master ' s Degree Thesis Development of a 3D printed Micro. (2020).
94. Udroiu, R. & Braga, I. C. Polyjet technology applications for rapid tooling. *MATEC Web Conf.* **112**, 03011 (2017).
95. FE-SEM. https://www.zeiss.com/microscopy/int/products/scanning-electron-microscopes/geminisem.html.